# Semi-infinite anisotropic spherical model: Correlations at $T \geqslant T_c$

D. A. Garanin*
*Max-Planck-Institut für Physik Komplexer Systeme, Nöthnitzer Strasse 38, D-01187 Dresden, Germany*
(Received 12 February 1998)

The ordinary surface magnetic phase transition is studied for the exactly solvable anisotropic spherical model (ASM), which is the limit $D \to \infty$ of the $D$-component uniaxially anisotropic classical vector model. The bulk limit of the ASM is similar to that of the spherical model, apart from the role of the anisotropy stabilizing ordering for low lattice dimensions, $d \leqslant 2$, at finite temperatures. The correlation functions and the energy density profile in the semi-infinite ASM are calculated analytically and numerically for $T \geqslant T_c$ and $1 \leqslant d \leqslant \infty$. Since the lattice dimensionalities $d=1$, 2, 3, and 4 are special, a continuous spatial dimensionality $d'=d-1$ has been introduced for dimensions parallel to the surface. However, preserving a discrete layer structure perpendicular to the surface avoids unphysical surface singularities and allows numerical solitions that reveal significant short-range features near the surface. The results obtained generalize the isotropic-criticality results for $2<d<4$ of Bray and Moore [Phys. Rev. Lett. **38**, 735 (1977); J. Phys. A **10**, 1927 (1977)].
[S1063-651X(98)06607-0]

PACS number(s): 64.60.Cn, 75.10.Hk, 75.30.Pd

## I. INTRODUCTION

Magnetic ordering in semi-infinite and film geometries is an old problem currently receiving increasing attention because of enormous progress in fabrication of magnetic structures on the atomic scale. Theoretical methods using the mean-field approximation (MFA) or the phenomenological Landau theory [1–5] provided classification and description of the qualitative features of different types of surface phase transitions. High-temperature series expansions [4] and Monte Carlo simulations [6], as well as the scaling analysis [4,7] and the $\epsilon$ expansion [8–10], shed light on the details of the surface critical behavior. A general review of these approaches can be found in Refs. [11,12]. Examples of recent work in film geometry based on $\epsilon$ expansion are Refs. [13,14]. A special case is the confined two-dimensional Ising ($S=\frac{1}{2}$) model, for which exact solutions have been found [15–18].

The ordinary surface phase transition of the semi-infinite ferromagnet occurs at the bulk critical temperature $T_c$. It is characterized by a number of surface critical exponents the definition of which can be found in Ref. [11]. In particular, the susceptibilities at the surface with respect to the fields applied either in the bulk or at the surface are described by the exponents $\gamma_1$ and $\gamma_{11}$, respectively, which in the MFA are given by $\gamma_1=\frac{1}{2}$ and $\gamma_{11}=-\frac{1}{2}$ (no divergence), in contrast to the bulk exponent $\gamma=1$. In thin films, which are more important for applications and more interesting for the experiment, there are additional effects, such as the lowering of $T_c$ in comparison to its bulk value and the crossover between the three- and two-dimensional behavior as a function of the film thickness $L$ [19–21].

The main body of the theoretical work on surface phase transitions is being done, with an exclusion of the $2d$ Ising model, starting from the field-theoretical continuous Hamiltonians or free energies. Such an approach has proven to be very useful for establishing the universality classes and critical laws but, on the other hand, the (nonuniversal) absolute values of observables, such as critical amplitudes, remain undetermined. In addition to the restrictions of the field-theoretical methods that are well known from bulk physics, there are more specific problems related to the role of the lattice discreteness in confined geometries. One can question how the continuous approach can be applied to thin films consisting of a *mesoscopic* number of layers. A similar question can be addressed to the semi-infinite ferromagnets as well—does the continuous approximation apply in the region near the boundary, $n \sim 1$, where $n=1,2,\ldots$ is the layer number? The MFA, or the Landau theory, gives a positive answer to this question near criticality, where the correlation length $\xi_c$ is much larger than the lattice spacing $a_0$, and the order parameter—the magnetization—cannot change at distances smaller than $\xi_c$. This is, however, not the case if one goes beyond the MFA and considers spin-spin correlation functions. If the temperature is high enough, or the system is classical, spin waves with the wave vectors up to the edge of the Brillouin zone $k \sim k_{\max}=\pi/a_0$ are excited. This means that correlation functions comprise $a_0$ as the length parameter, additionally to $\xi_c$, and thus there can be inhomogeneities near the surface of a ferromagnet on the scale of several atomic layers, even near criticality. This boundary region, $n \sim 1$, is that which can be locally probed in experiments, and here the continuous approximation may become, at least quantitatively, wrong.

Spin-wave effects in weakly anisotropic systems drastically change their behavior in comparison to the MFA predictions. Magnetic models with continuous symmetry in low dimensions, $d \leqslant 2$, cannot order at finite temperatures, and for models with $d>2$ the correlation length is infinite in the whole region below $T_c$. These effects are not less important than the critical coupling of fluctuations giving rise to nonclassical critical indices. In Heisenberg systems the linear

*Permanent address: I. Institut für Theoretische Physik, Universität Hamburg, Jungius Strasse 9, D-20355 Hamburg, Germany. Electronic addresses: garanin@mpipks-dresden.mpg.de, garanin@physnet.uni-hamburg.de

 

spin-wave theory satisfactorily describes the above mentioned effects well below $T_c$ but breaks down at elevated temperatures. There is, however, a model where a kind of spin-wave description is valid in the whole temperature range, whereas the critical fluctuation coupling vanishes. This is the $D$-component classical spin vector model proposed by Stanley [22,23] in the limit $D\to\infty$. Stanley has shown [24] that in this limit the partition function of a homogeneous ferromagnet coincides with that of the spherical model (SM). The latter was advanced by Berlin and Kac [25] as an exactly solvable substitute for the Ising model. The formalism contains, however, the spin-wave integral over the Brillouin zone and describes rather the properties of the isotropic Heisenberg model. The spherical model in its traditional form was extended to inhomogeneous systems by Barber and Fisher [26], who found a nonmonotonic dependence $T_c(L)$ for thin films. This unexpected feature was attributed to the failure of the global spin constraint in the inhomogeneous case. Later, an improved version of the SM was proposed, which used spin constraints on each lattice site [27], and it was shown that this version is equivalent to the $D=\infty$ model in the inhomogeneous case. Application of the SM with constraints in each layer [28] yielded a reasonable monotonic dependence of the numerically calculated $T_c(L)$ for the films in four dimensions. Because of the complexity of models of this type, most researchers still use the more convenient global-constraint SM in confined geometries (see, e.g., Refs. [29–31]). Very recently, a compromised model was proposed [32], which uses a constraint for the spins at the surface in addition to that for the bulk ones. The properties of such a model are closer, in a sense, to those of the SM with the local spin constraint and, hence, to those of the $D=\infty$, or $O(\infty)$, model.

A remarkable property of the Stanley model is that it can be easily extended to the anisotropic case, whereas the traditional SM cannot. This is very important because the anisotropy breaking a continuous symmetry plays a crucial role in low-dimensional systems, where it stabilizes ordering at finite temperatures. The limit $D\to\infty$ of the uniaxial $D$-component vector model determines the so-called anisotropic spherical model (ASM), which is described in the inhomogeneous case by a closed set of equations for the variables on the lattice sites obtained in Ref. [33]. The ASM was applied in Ref. [34] to study the dependence $T_c(L)$ for ferromagnetic films in three dimensions. Here, for all fixed values of the film thickness $L$ one has $T_c\to 0$ in the isotropic limit because of the two-dimensionality of the film, and such a behavior is pertinent for any Heisenberg film with finite $D$ as well. Thus, allowing for the anisotropy is relevant here, and it cannot be done within the traditional SM. An interesting feature of the solution obtained in Ref. [34] is the role of the correlation length of the transverse spin components, $\xi_{c\alpha}$, in the crossover from the three- to two-dimensional behavior of the film, which takes place for $L\lesssim\xi_{c\alpha}$. Note that in the finite-size scaling analysis (see, e.g., Ref. [11]) only the diverging longitudinal correlation length $\xi_{cz}$ is used, whereas the noncritical transverse correlation length is disregarded as an irrelevant variable.

Another application of the ASM is to the temperature-driven phase transition between the Bloch and linear (Ising-like) domain walls in uniaxial ferromagnets at some $T_B<T_c$ [33]. This phase transition was studied within the framework of the MFA and the Landau theory in Refs. [35–39] and with a field-theoretical method in Ref. [40]. A low minimum of the domain-wall mobility at $T_B$ predicted in Refs. [41,42] was used to identify the domain-wall phase transition in the dynamic susceptibility experiments on Ba and Sr hexaferrites [43,44]. It is clear that the anisotropy is an important characteristic of the model, giving rise to the very existence of domain walls of *finite width* separating the ''up'' and ''down'' domains. For this reason, the attempts to describe domain walls with the traditional SM in both versions with [45] and without [46] the global spin constraint could not yield relevant results.

In the recent work of Ref. [47] it was shown that the ASM and SM are *not* equivalent, even in the isotropic homogeneous case, if the longitudinal correlation function (CF) $S_{zz}(\mathbf{k})$ below $T_c$ is involved. Whereas in the traditional SM the CF is proportional to $1/k^2$ at small wave vectors, the behavior of $S_{zz}(\mathbf{k})$ in the ASM shows a more complicated behavior governed by the spin-wave effects and is sensitive to the dimensionality. In three dimensions, $S_{zz}(\mathbf{k})\propto 1/k$, which is familiar from the linear spin-wave theory. The above law holds for $k\lesssim\kappa_m\propto T_c-T$, i.e., there is a critical length scale $\xi_m=1/\kappa_m$ in the theory. The length $\xi_m$ is analogous to the ''bare,'' or the mean-field, correlation length below $T_c$, whereas the true longitudinal correlation length $\xi_{cz}$ remains infinite in the isotropic model below $T_c$. The former is responsible for the crossover of the real-space CF from $S_{zz}(\mathbf{r})\propto 1/r$ for $r\lesssim\xi_m$ to $S_{zz}(\mathbf{r})\propto 1/r^2$ for $r\gtrsim\xi_m$.

The ASM equations of Ref. [33], as well as those for the SM without the global spin constraint [28], are rather complicated, strongly nonlinear equations for the variables on a lattice. In the latter case some researchers termed them analytically intractable. Nevertheless, for the weakly anisotropic ASM in the domain-wall geometry it was possible to guess the solution [33], which yielded an example of a phase transition of an interface that is analytically tractable beyond the MFA. Surfaces with free boundary conditions make the problem much more complicated. In Ref. [34] only the most important and partially rough asymptotes for the $T_c$ shift in films could be obtained, and numerical calculations have not been performed. The aim of this work is to investigate the influence of surfaces on magnetic ordering in more detail for the ordinary phase transition in the semi-infinite ASM in the temperature range $T\geqslant T_c$. As we shall see, analytical solutions are available in the dimensionality ranges $1\leqslant d\leqslant 2$ and $d\geqslant 4$, as well as for $2<d<4$, both at and away from the isotropic criticality. In addition, the problem will be solved numerically in all the relevant cases.

The same problem presented here was addressed in the seminal work by Bray and Moore [48], who considered a field theory with the volume and surface Hamiltonian densities of the type $(\nabla\phi)^2+\tau\phi^2+u\phi^4$ and $c\phi^2$, respectively, for the $n$-component vector order parameter $\phi$ in the limit $n\to\infty$. Since this model is isotropic, the range $1\leqslant d\leqslant 2$ is excluded from the outset due to the absence of ordering in the bulk. For $2<d<4$ a very important solution for the correlation function at criticality was obtained, however, only for the ''magic'' $d$-dependent values $u^*(d)$ of the coupling constant $u$. This solution yielded the anomalous dimensions $\eta_\parallel=d-2$ and $\eta_\perp=(d-2)/2$, with which all other surface

critical indices could be derived from the scaling arguments (see, e.g., Refs. [11,12]). These critical indices depend on $d$ and differ from the mean-field ones, as well as from those of the global-constraint semi-infinite SM. In the solution of Bray and Moore the required coupling constant $u^*(d)$ vanishes for $d=4$, i.e., the model simplifies to the exactly solvable and trivial Gaussian model showing the mean-field behavior. On one hand, it seems reasonable, because the critical indices indeed simplify to their mean-field values for $d>4$. On the other hand, one could desire more detailed information about the critical behavior of the models with $u\neq u^*$, in particular for $u\neq 0$ and $d>4$. Unfortunately, no extension of the analytical results of Bray and Moore in this direction, or for the off-criticality case, is possible. Also a numerical solution is hampered for this model by insurmountable difficulties. Apart from the obvious impossibility of handling the inhomogeneities on the scale of the lattice spacing with a continuous-field theory, it turns out that this model cannot be solved numerically at all because near the surface, where the boundary condition is set, the continuous approximation does not apply. In fact, this is an example of a situation in which using a field-theoretical approach in statistical mechanics brings only disadvantages. By contrast, the ASM formulated from the beginning in its true form on a lattice leads to the ASM equations which are well defined and suitable for numerical solution, and also can be considered continuously far from the surface.

The main body of the article is organized as follows. In Sec. II the system of equations describing the ASM in zero field is written down. Its bulk solution, which differs from the well known solution for the spherical model by the incorporating the uniaxial anisotropy, is studied for all lattice dimensions. The quantity playing the central role in the theory, the gap parameter $G_n$, is related to the reduced energy density $\tilde{U}_n$. The continued-fraction formalism, which is mainly needed for the numerical solution of the ASM system of equations, is described. Section II concludes with the results for the variation of $G_n$ far above and far below $T_c$. In Sec. III the ASM is solved analytically in low $(1\leqslant d\leqslant 2)$ and high $(4\leqslant d)$ lattice dimensions, starting from the exact solution for the one-dimensional ''toy'' model. The energy density profiles and spin correlation functions are calculated analytically in all possible cases. In Sec. IV the most interesting case $2<d<4$ is investigated. Analytical solutions are obtained for the isotropic model at criticality and away from the isotropic criticality. In Sec. V the semi-infinite ASM is numerically solved in the whole range of dimensions at $T\geqslant T_c$. The results for the energy density profile and correlation functions are presented. In Sec. VI the main results of the paper are summarized and compared with the results of other approaches.

## II. BASIC RELATIONS

### A. ASM equations

We start from the Hamiltonian of the uniaxially-anisotropic classical $D$-vector model, which, in the absence of the magnetic field, can be written in the form

$$\mathcal{H}=-\frac{1}{2}\sum_{ij} J_{ij}\left( m_{zi}m_{zj}+\eta\sum_{\alpha=2}^{D} m_{\alpha i}m_{\alpha j}\right), \qquad (2.1)$$

where $\mathbf{m}_i$ is the normalized $D$-component vector, $|\mathbf{m}_i|=1$, and $\eta\leqslant 1$ is the dimensionless anisotropy factor. In the mean-field approximation, the Curie temperature of this model is $T_c^{\mathrm{MFA}}=J_0/D$, where $J_0$ is the zero Fourier component of the exchange interaction. It is convenient to use $T_c^{\mathrm{MFA}}$ as the energy scale and introduce the dimensionless temperature variable $\theta\equiv T/T_c^{\mathrm{MFA}}$. Using the diagram technique for classical spin systems [49,50], in the limit $D\to\infty$ one arrives at the closed system of Eqs. (33) for the average magnetization $m_i\equiv\langle m_{zi}\rangle$ and the correlation function of transverse $(\alpha\geqslant 2)$ spin components: $s_{ij}\equiv D\langle m_{\alpha i}m_{\alpha j}\rangle$. This system of equations describing the anisotropic spherical model consists of the magnetization equation

$$m_i=G_i\sum_j \lambda_{ij}m_j, \qquad (2.2)$$

the Dyson equation for the transverse CF

$$s_{ii'}=\theta G_i\delta_{ii'}+\eta G_i\sum_j \lambda_{ij}s_{ji'}, \qquad (2.3)$$

and the kinematic relation playing the role of the spin constraint on a lattice site $i$,

$$s_{ii}+m_i^2=1. \qquad (2.4)$$

Here $\delta_{ij}$ is the site Kronecker symbol, $\lambda_{ij}\equiv J_{ij}/J_0$, and the so-called gap parameter $G_i$ is the one-site cumulant spin average $D\langle m_{\alpha i}m_{\alpha i}\rangle_{\mathrm{cum}}/\theta$ renormalized by Gaussian fluctuations. We will see below that $G_i$ can be related to the energy density at the site $i$.

The ASM system of equations is self-consistent. It is instructive to compare it with the MFA equations that can be recovered via the following steps. (i) Ignore correlations in Eq. (2.3), which leads to $s_{ii}=\theta G_i$. (ii) Express $G_i$ through $m_i$ with the help of Eq. (2.4) to get $G_i=(1-m_i^2)/\theta$. (iii) Insert the latter into Eq. (2.2) to obtain the closed equation for magnetization. The form of the latter is simplified with respect to the general-$D$ case because of the simplification of the Langevin function in the limit $D\to\infty$. The resulting $m_i$ is zero above $\theta_c=1$ and nonzero below $\theta_c$. (iv) With $G_i$ determined, which is simply $G_i=1/\theta$ for $\theta\geqslant\theta_c$, return to Eq. (2.3) to find the improved correlation function. It is clear in step (iv) that the MFA is not self-consistent, even in the simpler case above $\theta_c$. This is the reason why the MFA value of $\theta_c$ found from the CF equation (2.3) with $G_i=1/\theta$ for the spatially homogeneous isotropic low-dimensional magnets is nonzero, in contradiction with the result of more rigorous approaches. By contrast, the ASM equations are free from such an inconsistency and they correctly describe the dimensional effects in isotropic and weakly anisotropic systems. It should be noted that in the ''Ising limit'' $\eta=0$ all the steps above leading to the MFA equations are exact, i.e., the classical Ising model in the limit $D\to\infty$ is exactly described by the mean-field approximation.

For the model with the nearest-neighbor interaction $J_{ij}$ on the $d$-dimensional hypercubic lattice in the semi-infinite geometry, it is convenient to use the Fourier representation in $d'=d-1$ translationally invariant dimensions parallel to the surface and the site representation in the $d$th dimension. The

Dyson equation (2.3) for the Fourier-transformed CF $\sigma_{nn'}(\mathbf{q})$ then takes the form of a system of the second-order finite-difference equations in the set of layers $n=1,2,\ldots,\infty$,

$$2b_n\sigma_{nn'}-\sigma_{n+1,n'}-\sigma_{n-1,n'}=(2d\theta/\eta)\delta_{nn'}. \quad (2.5)$$

$b_n$ here is given by

$$b_n=1+d[(\eta G_n)^{-1}-1]+d'(1-\lambda'_{\mathbf{q}}), \quad (2.6)$$

where $\lambda'_{\mathbf{q}}$ is given by

$$\lambda'_{\mathbf{q}}=\frac{1}{d'}\sum_{i=1}^{d'}\cos(q_i) \quad (2.7)$$

and the lattice spacing $a_0$ is set to unity. The magnetization equation (2.2) takes the form

$$2\overline{b}_n m_n-m_{n+1}-m_{n-1}=0, \quad (2.8)$$

with $\overline{b}_n=1+d[G_n^{-1}-1]$. Since the layer with $n=0$ is absent, one can use

$$\sigma_{0n'}=0, \quad m_0=0 \quad (2.9)$$

as the free boundary conditions to Eqs.(2.5) and (2.8). If the interaction in the boundary layer differs from that in the bulk (see, e.g., Ref. [11]) the form of the boundary conditions changes. The constraint equations (2.4) can now be written as

$$s_{nn}+m_n^2=1, \quad s_{nn}=\int\frac{d^{d'}\mathbf{q}}{(2\pi)^{d'}}\sigma_{nn}(\mathbf{q}). \quad (2.10)$$

For $n\gg 1$, $q\ll 1$, and $\kappa\ll 1$, where $\kappa$ is the inverse transverse correlation length defined by (2.34) below, the second-order finite-difference CF equation (2.5) simplifies to the differential equation for the Green's function

$$\left(\frac{d^2}{dn^2}-\tilde{q}^2+2dG_{1n}\right)\sigma_{nn'}=-2d\theta\delta(n-n'), \quad (2.11)$$

where $n$ is regarded as a continuous variable, $\tilde{q}\equiv\sqrt{\kappa^2+q^2}$, and

$$G_{1n}\equiv G_n-G\ll 1 \quad (2.12)$$

is the deviation of the gap parameter from its bulk value $G$. The magnetization equation (2.8) takes on a similar form with $\tilde{q}\Rightarrow 0$ and without the inhomogeneous term.

Before proceeding, let us consider the solution of equations (2.5) for the important special variation of $G_n$ near the surface, in which only $G_1$ may differ from the bulk value $G$. In this case one can solve Eq. (2.5) directly with the result

$$\sigma_{nn'}=\frac{d\theta/\eta}{\sqrt{b^2-1}}\left[\alpha^{|n-n'|}-\alpha^{n+n'-2}\frac{\alpha-2b_{11}}{\alpha^{-1}-2b_{11}}\right], \quad (2.13)$$

where $\alpha\equiv b-\sqrt{b^2-1}$, $b$ is the bulk value of $b_n$, and $b_{11}\equiv b-b_1$. One of the particular cases of (2.13) is $b_{11}=0$, which corresponds to the MFA or to the high-dimensional ($d\geqslant 4$) lattices for $n\gg 1$ (see Sec. III C). Here Eq. (2.13) simplifies to

$$\sigma_{nn'}=\frac{d\theta/\eta}{\sqrt{b^2-1}}[\alpha^{|n-n'|}-\alpha^{n+n'}]. \quad (2.14)$$

Another particular case is $G_1=[2d/(2d-1)]G$, i.e., $2b_{11}=1$. As we shall see below, a variation of $G_n$ close to this one is realized for low-dimensional ($d\leqslant 2$) lattices in the weakly anisotropic case at low temperatures. Here (2.13) reduces to

$$\sigma_{nn'}=\frac{d\theta/\eta}{\sqrt{b^2-1}}[\alpha^{|n-n'|}+\alpha^{n+n'-1}]. \quad (2.15)$$

For $1-\eta\ll 1$ and $\tilde{q}\ll 1$ one can define $2b_{11}\cong 1-c$ and simplify Eq. (2.13) to

$$\sigma_{nn'}\cong\frac{d\theta}{\tilde{q}}[e^{-\tilde{q}|n-n'|}+f(\tilde{q})e^{-\tilde{q}(n+n'-2)}], \quad (2.16)$$

with $f(\tilde{q})=(\tilde{q}-c)/(\tilde{q}+c)$. This result could also be obtained solving the differential equation (2.11) with the boundary condition

$$\left[c\sigma_{nn'}-\frac{d}{dn}\sigma_{nn'}\right]_{n=1}=0 \quad (2.17)$$

following from Eq. (2.9). The remarkable feature of this solution is that it becomes insensitive to the exact form of the boundary condition if $\tilde{q}\ll c$ or $\tilde{q}\gg c$. In fact, as will be argued below, the limiting forms of $\sigma_{nn'}$ with both signs of the surface-induced term, (2.14) and (2.15), are realized for more general variations of $G_n$, in which $G_n$ differs from the bulk value in some localized region near the surface, $n\lesssim n^*$.

Note that the quantity $c$ above is similar to the coefficient in the surface-energy term that is introduced in the phenomenological field theory of phase transitions and it defines the extrapolation length $c=\lambda_e^{-1}$ (see, e.g., Ref. [11]). This term was used, in particular, by Bray and Moore [48], who have set $c=\infty$ for the ordinary phase transition to remove the uncertainty. We shall see, however, that the weakly anisotropic models with $d\leqslant 4$ the microscopic solution is characterized by effective values of $c$ of order $\kappa\ll 1$, i.e., by large extrapolation lengths.

The equation for the longitudinal correlation function, $\sigma^{zz}_{nn'}$, is not coupled to the ASM system of equations, since fluctuations of the (only one) longitudinal spin component make contributions of order $1/D$ to the physical quantities, which disappear in the spherical limit. Above $T_c$ in zero field this equation has the form (2.5) with $\eta=1$. The latter amounts to replacing $\tilde{q}\Rightarrow\tilde{q}_z\equiv\sqrt{\kappa_z^2+q^2}$ in (2.11), where $\kappa_z$ is the inverse longitudinal correlation length defined by Eq. (2.48) below. Thus both $\sigma_{nn'}$ and $\sigma^{zz}_{nn'}$ are given by the same function of different arguments, and the latter is more convenient, since its argument spans the wider range, starting

from zero at criticality ($\kappa_z=0$). In this limit, $\tilde{q}_z=0$, formula (2.16) for $\sigma_{nn}^{zz}$ reduces to the expression

$$\sigma_{nn}^{zz}\cong 2d\theta(n-1+\lambda_e), \tag{2.18}$$

where the extrapolation length $\lambda_e$ is given by $\lambda_e=1/c$.

### B. Energy and susceptibilities

For the ferromagnetic model described by the Hamiltonian (2.1), the energy corresponding to the $i$th site, $U_i$, is determined in the spherical limit $D\to\infty$ by the spontaneous magnetization $m_i\equiv\langle m_{zi}\rangle$ and the transverse CF $s_{ij}$:

$$U_i=-\frac{1}{2}\sum_j J_{ij}m_i m_j-\frac{\eta}{2}\sum_j J_{ij}s_{ij}. \tag{2.19}$$

It is convenient to consider the reduced energies $\tilde{U}\equiv U/|U_0|$ where $U_0=-J_0/2$ is the ground-state energy. In the semi-infinite geometry the reduced energy corresponding to any site in the $n$th layer can be written as

$$\tilde{U}_n=2d'\tilde{U}_{nn}+\tilde{U}_{n,n-1}+\tilde{U}_{n,n+1}, \tag{2.20}$$

where $\tilde{U}_{nn}$ is due to the interaction with one of the neighbors in the same layer and $\tilde{U}_{n,n\pm1}$ is due to that with the neighbors in the adjacent layers. The terms of Eq. (2.20) can be represented through magnetization and the layer CF $\sigma_{nn'}(\mathbf{q})$ as

$$\tilde{U}_{nn}=-\frac{1}{2d}\left[m_n^2+\int\frac{d^{d'}\mathbf{q}}{(2\pi)^{d'}}\eta\lambda'_{\mathbf{q}}\sigma_{nn}(\mathbf{q})\right], \tag{2.21}$$

$$\tilde{U}_{n,n\pm1}=-\frac{1}{2d}\left[m_n m_{n\pm1}+\int\frac{d^{d'}\mathbf{q}}{(2\pi)^{d'}}\eta\sigma_{n,n\pm1}(\mathbf{q})\right].$$

In practice, only the total energy of the site $\tilde{U}_n$ is needed. Using the CF equation (2.5) to eliminate $\sigma_{n,n\pm1}$ and the magnetization equation (2.8) to eliminate $m_{n\pm1}$ in Eq. (2.21), one comes to the remarkably simple result

$$\tilde{U}_n=\theta-1/G_n. \tag{2.22}$$

The deviation of the energy density from the bulk density $\tilde{U}$ is given by

$$\tilde{U}_{1n}\equiv\tilde{U}_n-\tilde{U}\cong G_{1n}/G^2, \tag{2.23}$$

where $G_{1n}$ is defined by (2.12). This formula provides additional physical interpretation of $G_{1n}$, besides that following from the role it plays in the correlation functions (see Sec. II C).

The susceptibilities of a ferromagnet are related to the correlation functions. In the semi-infinite geometry the generic susceptibility is that describing the response of the spin polarization in the $n$th layer to the dimensionless magnetic field $\mathbf{h}\equiv J_0\mathbf{H}$ in the $n'$th one. In the region above $T_c$ which is considered throughout the paper, it can be written as

$$\chi_{\alpha nn'}=\partial\langle m_{\alpha n}\rangle/\partial h_{\alpha n'}=\sigma_{nn'}^{\alpha\alpha}(0)/\theta. \tag{2.24}$$

Here, in the anisotropic case the longitudinal ($\alpha=1=z$) and transverse ($\alpha\neq1=z$) susceptibilities are different. For the transverse susceptibility the corresponding layer correlation function $\sigma_{nn'}(0)$ (the index $\alpha$ is dropped for convenience) is determined by the system of linear equations (2.5). The longitudinal layer CF $\sigma_{nn'}^{zz}(0)$ satisfies the same system of equations with $\eta\Rightarrow1$ in (2.6). The most important of the susceptibilities (2.24) is $\chi_{\alpha11}$, corresponding to the boundary layer. Whereas for $\eta<1$ the transverse susceptibility $\chi_{11}$ is noncritical, the longitudinal one $\chi_{z11}$ shows critical behavior with the critical index $\gamma_{11}$. One can also consider the response in the $n$th layer to the homogeneous field. The appropriate susceptibilities are given by

$$\chi_{\alpha n}=\frac{\partial\langle m_{\alpha n}\rangle}{\partial h_\alpha}=\sum_{n'=1}^{\infty}\chi_{\alpha nn'}=\frac{1}{\theta}\sum_{n'=1}^{\infty}\sigma_{nn'}^{\alpha\alpha}(0). \tag{2.25}$$

### C. Bulk limit and continuous dimensions

In the homogeneous case, $m_i=m$ and $G_i=G$ are constants, and the equation (2.3) can be easily solved with the help of the Fourier transformation. This yields the Fourier-transformed transverse CF

$$s(\mathbf{k})=\frac{\theta G}{1-\eta G\lambda_{\mathbf{k}}}. \tag{2.26}$$

The longitudinal CF $s_{zz}(\mathbf{k})$ is given above $T_c$ by the same expression with $\eta=1$. Now the autocorrelation function $s_{ii}$ can be expressed as

$$s_{ii}=\int\frac{d^d\mathbf{k}}{(2\pi)^d}s(\mathbf{k})=\theta GP(\eta G)=1-m^2, \tag{2.27}$$

where

$$P(X)\equiv\int\frac{d^d\mathbf{k}}{(2\pi)^d}\frac{1}{1-X\lambda_{\mathbf{k}}} \tag{2.28}$$

is the lattice Green's function. The quantity $\lambda_{\mathbf{k}}\equiv J_{\mathbf{k}}/J_0$ is given for the nearest-neighbor (nn) interaction by Eq. (2.7) with $d'\Rightarrow d$. The total wave vector $\mathbf{k}$ is related to $\mathbf{q}$ above by $\mathbf{k}=k_z\mathbf{e}_z+\mathbf{q}$, where $\mathbf{q}\cdot\mathbf{e}_z=0$. The last equation in (2.27) together with the equation

$$m(1-G)=0 \tag{2.29}$$

following from (2.2) in the homogeneous case completely describes the ASM in zero magnetic field $H$. The homogeneous ASM equations for $H\neq0$ can be found in Refs. [49,51]. The lattice integral $P(X)$ has the following properties:

$$P(X)\cong\begin{cases}1+X^2/(2d), & X\ll 1\\ 1/(1-X^2)^{1/2}, & d=1\\ (1/\pi)\ln(8/X_1), & X_1\ll 1,\quad d=2\\ W_3-cX_1^{1/2}, & X_1\ll 1,\quad d=3\\ W_4-cX_1\ln(c'/X_1), & X_1\ll 1,\quad d=4\\ W_d-cX_1, & X_1\ll 1,\quad d>4,\end{cases} \tag{2.30}$$

where $X_1\equiv 1-X$ and $W_3=1.51639$, $W_4=1.23947$, $W_5=1.15631$, etc., are the Watson integrals. Since above $T_c$ the constraint equation (2.4) yields $s_{ii}=1$, Eq. (2.27) determines the value of $G$ which increases with decreasing temperature. The high-temperature asymptote of $G$ is $G\cong\theta^{-1}[1-\eta^2\theta^{-2}/(2d)]$, $\theta\gg 1$. This results in $\tilde{U}\cong-\eta^2/(2d\theta)$ for the energy in the bulk, which is given by Eq. (2.22) with $n\to\infty$. The criticality is determined by $G=1$, which corresponds to closing the gap in the longitudinal correlation function $s_{zz}(\mathbf{k})$ [see Eq. (2.26)]. This is the reason for calling $G$ the ''gap parameter.'' Below $\theta_c$ one obtains $G=1$ from Eq. (2.29) and then

$$m=\sqrt{1-\theta/\theta_c},\quad \theta_c=1/P(\eta) \tag{2.31}$$

from Eq. (2.27). Here the value of the Curie temperature $\theta_c$ [49] generalizes the well-known result of the spherical model $\theta_c=1/W$ [25] for the anisotropic case.

The influence of the anisotropy on the ordering in the ASM is rather essential. The anisotropic gap in the transverse CF $s(\mathbf{k})$ prevents long-wavelength excitations (transverse fluctuations) from destroying the long-range order in two dimensions, and $\theta_c$ determined by Eq. (2.31) is finite for $\eta<1$. Moreover, the phase transition at finite temperature occurs even in the *one-dimensional* ASM. This surprising result is due to the switching off of the *longitudinal* fluctuations in the limit $D\to\infty$, which are responsible for the breakdown of the long-range order in one dimension.

The bulk solution of the linear system of equations (2.5) has the form

$$\sigma^{\rm bulk}_{nn'}(\mathbf{q})=\frac{d\theta}{\eta}\frac{\alpha^{|n-n'|}}{\sqrt{b^2-1}},\quad \alpha\equiv b-\sqrt{b^2-1}, \tag{2.32}$$

where $b$ is given by (2.6) with $G_n\Rightarrow G$. This result could also be obtained by the integration of the bulk transverse CF $s(\mathbf{k})$ given by Eq. (2.26) over $k_z$. For the weakly anisotropic ASM, $1-\eta\ll 1$, at small wave vectors the transverse correlation functions in the bulk, Eqs. (2.26) and (2.32), have the form

$$s(\mathbf{k})\cong\frac{2d\theta}{\kappa^2+k^2},\quad \sigma^{\rm bulk}_{nn}(\mathbf{q})=\frac{d\theta}{\sqrt{\kappa^2+q^2}}, \tag{2.33}$$

where $\kappa$ is defined by

$$\kappa^2\equiv 2d[1/(\eta G)-1]\cong 2d[1-\eta G]\ll 1. \tag{2.34}$$

One can see that the transverse correlation length $\xi_{c\alpha}\equiv 1/\kappa$ increases without diverging with decreasing temperature down to $\theta_c$ and remains constant below $\theta_c$, in accordance with the behavior of $G$.

The field-theoretical multiple-component $\phi^4$ model used by Bray and Moore [48] extends in a natural way for arbitrary noninteger lattice dimensions $d$. The discrete structure of the lattice which is important near the surface is, however, lost in such a model. A better way to get a continuous-dimension model to study crossover between different lattice dimensions is to consider the $d'$ translationally invariant dimensions as continuous, preserving the dimension $z$ perpendicular to the surface as discrete. This amounts to making the long-wavelength approximation

$$\lambda_{\mathbf{k}}=\frac{1}{d}\cos k_z+\frac{d'}{d}\lambda'_{\mathbf{q}},\quad \lambda'_{\mathbf{q}}\Rightarrow 1-\frac{q^2}{2d'} \tag{2.35}$$

*in the whole Brillouin zone* for the part of the expression for the exchange integral $J_{\mathbf{k}}=J_0\lambda_{\mathbf{k}}$. The natural hypercubic cutoff $|k_i|\leqslant\pi$ and the corresponding density of states are modified for the $\mathbf{q}$ components according to

$$\int\frac{d^{d'}\mathbf{q}}{(2\pi)^{d'}}\ldots\Rightarrow\frac{d'}{\Lambda^{d'}}\int_0^{\Lambda}dqq^{d'-1}\ldots \tag{2.36}$$

with $\Lambda=\sqrt{2(d+1)}$. One can check that the sum rules

$$\int_{-\pi}^{\pi}\frac{dk_z}{2\pi}\frac{d'}{\Lambda^{d'}}\int_0^{\Lambda}dqq^{d'-1}\begin{Bmatrix}1\\ \lambda_{\mathbf{k}}\end{Bmatrix}=\begin{Bmatrix}1\\ 0\end{Bmatrix} \tag{2.37}$$

are satisfied. Now using (2.32), one can, instead of (2.27), write

$$\frac{d'}{\Lambda^{d'}}\int_0^{\Lambda}dqq^{d'-1}\frac{d\theta}{\eta}\frac{1}{\sqrt{b^2-1}}=\theta GP(\eta G), \tag{2.38}$$

which is the definition of $P(X)$ in our continuous-dimension model. The resulting $P(X)$ posesses the same general properties (2.30). The Watson integrals $W$ for some values of $d$ are $W_{2.5}=2.527059$, $W_{3.0}=1.719324$, $W_{4.0}=1.321825$, and $W_{5.0}=1.192848$.

For both hypercubic and continuous-dimension lattices the singular behavior of the integral $P(X)$ for $\kappa\ll 1$ is described by

$$P(X)\cong\begin{cases}C_d/\kappa^{2-d}, & 1\leqslant d\leqslant 2\\ W-C_d\kappa^{d-2}, & 2<d<4.\end{cases} \tag{2.39}$$

Here $C_d=A_d\times dM_d$, where the nonuniversal factor $A_d$ reads

$$A_d\equiv\begin{cases}S_{d'}/(2\pi)^{d'}, & \text{hypercubic lattice}\\ d'/\Lambda^{d'}, & \text{continuous dimensions}\end{cases} \tag{2.40}$$

and $S_d=2\pi^{d/2}/\Gamma(d/2)$ is the surface of the $d$-dimensional unit sphere. The universal quantity $M_d$ which will be needed below is given by

$$M_d\equiv\int_0^{\Lambda/\kappa}\frac{dyy^{d'-1}}{\sqrt{1+y^2}}=\frac{1-\kappa^{2-d}}{2\pi^{1/2}}\Gamma\left(\frac{d-1}{2}\right)\Gamma\left(\frac{2-d}{2}\right) \tag{2.41}$$

for $d\leqslant 2$ and

$$M_d \equiv \int_0^\infty dy\ y^{d'-1}\left[\frac{1}{y}-\frac{1}{\sqrt{1+y^2}}\right]$$

$$=\frac{\pi}{\cos(\pi\mu)}\frac{\Gamma(d-1)}{2^{d-1}\Gamma^2(d/2)}$$

$$\mu \equiv \frac{d-3}{2} \tag{2.42}$$

for $2<d<4$. The factor $1-\kappa^{2-d}$ in Eq. (2.41) is for $\kappa \ll 1$ close to unity if $d$ is not close to 2. It is needed for $2-d \ll 1$ to give

$$M_d \cong \frac{1-\kappa^{2-d}}{2-d} \cong \ln(1/\kappa) \tag{2.43}$$

with logarithmic accuracy. For $d \to 1$ one obtains $C_d \to 1$, in accordance with Eq. (2.30).

In the anisotropic case $\eta<1$, the value of $G$ determined from the equation $\theta G P(\eta G)=1$ approaches 1 linearly just above the Curie temperature $\theta_c$ given by Eq. (2.31):

$$1-G \cong \tau/I(\eta), \quad \tau \equiv \theta/\theta_c - 1, \tag{2.44}$$

where

$$I(X) \equiv 1+\frac{XP'(X)}{P(X)}, \quad P'(X) \equiv \frac{dP(X)}{dX}. \tag{2.45}$$

For the weakly anisotropic model this solution is valid in the narrow region defined by $1-G \ll 1-\eta$, i.e., below the crossover temperature $\tau^*=(1-\eta)I(\eta)$. For different lattice dimensions $\tau^*$ reads

$$\tau^* \sim \begin{cases} 1, & d<2 \\ 1/\ln[1/(1-\eta)], & d=2 \\ (1-\eta)^{(d-2)/2}, & 2<d<4 \\ (1-\eta)\ln[1/(1-\eta)], & d=4 \\ 1-\eta, & d>4. \end{cases} \tag{2.46}$$

For $\tau \gg \tau^*$ one has

$$1-G \sim \begin{cases} \theta^{2/(2-d)}, & d<2 \\ \exp(-A_d^{-1}/\theta), & d=2,\ 2.0 \\ \tau^{2/(d-2)}, & 2<d<4 \\ \tau/\ln\tau, & d=4 \\ \tau, & d>4, \end{cases} \tag{2.47}$$

where, according to Eq. (2.40), $A_2^{-1}=\pi$ and $A_{2.0}^{-1}=\sqrt{6}$. Here the result for $d \leqslant 2$ is valid for $\theta \ll 1$, i.e., a weakly anisotropic system can be close to criticality $(1-G \ll 1)$ in a temperature range extending far above $\theta_c \ll 1$. For $d \geqslant 2$ the Curie temperature $\theta_c$ is not small, and Eq. (2.47) requires $\tau \ll 1$.

The longitudinal CFs are given by the same formulas (2.33) and (2.34) with $\eta=1$ . The longitudinal correlation length $\xi_{cz} \equiv 1/\kappa_z$, where

$$\kappa_z^2 \equiv 2d[1/G-1] \cong 2d[1-G] \ll 1, \tag{2.48}$$

diverges at $\theta_c$ in different ways for the isotropic and anisotropic models according to Eqs. (2.44) and (2.47), respectively. The critical behavior of the ASM is, for $\eta<1$, in all respects analogous to that given by the mean-field approximation. This is due to the suppression of the singularity of the lattice Green's function $P(X)$ [see Eqs. (2.30) and (2.39)]. For $1-\eta \ll 1$ far enough from $\theta_c$, i.e., for $\tau \gg \tau^*$, the system behaves isotropically and, in particular, $\xi_{cz} \cong \xi_{c\alpha}$. Crossover at $\tau^*$ is analogous to that between the Heisenberg and Ising universality classes in the weakly anisotropic Heisenberg model. Here one has the crossover between the spherical and mean-field universality classes instead.

### D. Continued-fraction formalism

The linear homogeneous second-order finite-difference equation

$$2b_n \mathcal{Z}_n - \mathcal{Z}_{n+1} - \mathcal{Z}_{n-1} = 0, \tag{2.49}$$

which corresponds to the CF equation (2.5), has two linearly independent solutions, $\mathcal{I}_n$ and $\mathcal{K}_n$. They can be chosen so that $\mathcal{I}_n \to \infty$ and $\mathcal{K}_n \to 0$ for $n \to \infty$. The solution of Eq. (2.5) with the boundary condition (2.9) can be expressed through $\mathcal{I}_n$ and $\mathcal{K}_n$ as

$$\sigma_{nn'} = -\frac{2d\theta}{\eta \mathcal{W}_{n'}}\frac{2b_1\mathcal{I}_1-\mathcal{I}_2}{2b_1\mathcal{K}_1-\mathcal{K}_2}\mathcal{K}_n\mathcal{K}_{n'} + \frac{2d\theta}{\eta \mathcal{W}_{n'}}\begin{cases} \mathcal{I}_n\mathcal{K}_{n'}, & n \leqslant n' \\ \mathcal{I}_{n'}\mathcal{K}_n, & n' \leqslant n, \end{cases} \tag{2.50}$$

where the Wronskian $\mathcal{W}_n$ is given by

$$\mathcal{W}_n \equiv \mathcal{I}_n\mathcal{K}_{n-1} - \mathcal{K}_n\mathcal{I}_{n-1}. \tag{2.51}$$

It can be shown with the help of Eq. (2.49) that $\mathcal{W}_{n+1}=\mathcal{W}_n$, i.e., $\mathcal{W}_n$ is independent of $n$. It is convenient to redefine $\mathcal{I}_n$ by replacing it by its linear combination with $\mathcal{K}_n$, so that the redefined $\mathcal{I}_n$ satisfies the additional requirement $\mathcal{I}_0=0$ in the nonexisting layer $n=0$. This entails $2b_1\mathcal{I}_1-\mathcal{I}_2=0$, i.e., the first term in Eq. (2.50) becomes zero.

The solution (2.50) can be rewritten in the form of a continued fraction, which is appropriate in particular for numerical calculations. In terms of the functions $\alpha_n$ and $\alpha_n'$ determined by

$$\mathcal{I}_{n-1}/\mathcal{I}_n \equiv \alpha_n, \quad \mathcal{K}_{n-1}/\mathcal{K}_n \equiv 2b_n - \alpha_n' \tag{2.52}$$

the solution (2.50) for $n=n'$ becomes

$$\sigma_{nn} = \frac{2d\theta}{\eta}\frac{1}{2b_n-\alpha_n-\alpha_n'}. \tag{2.53}$$

The functions $\alpha_n$ and $\alpha_n'$ can be found from the forward and backward recurrence relations

$$\alpha_{n+1}=\frac{1}{2b_n-\alpha_n},\quad \alpha'_{n-1}=\frac{1}{2b_n-\alpha'_n}, \tag{2.54}$$

being the consequence of Eq. (2.49). The initial condition for the first one is $\alpha_1=0$. Far from the surface $\alpha_n$ approaches the bulk value $\alpha$ of Eq. (2.32). The backward relation for $\alpha'_n$ starts from $\alpha$ far from the surface. For numerical calculations in the isotropic case for $2<d<4$, a refined asymptote is needed (see the end of Sec. IV A). If the denominator of Eq. (2.53) becomes zero for $q=0$ (which is the case for the isotropic model at criticality for $2<d\leqslant 3$; see Sec. IV A), then with the help of Eq. (2.54) one can obtain the relation

$$\alpha_n\alpha'_{n-1}=1 \quad (q=0). \tag{2.55}$$

The general solution (2.50) can be represented through the diagonal Green function (2.53) via the relations

$$\sigma_{n,n-m}=\sigma_{n-m,n}=\alpha_{n-m+1}\alpha_{n-m+2}\ldots\alpha_n\sigma_{nn} \tag{2.56}$$

or, alternatively,

$$\sigma_{n+m,n}=\sigma_{n,n+m}=\alpha'_{n+m-1}\alpha'_{n+m-2}\ldots\alpha'_n\sigma_{nn}. \tag{2.57}$$

The consequence of these two relations is the useful formula

$$\sigma_{n,n+1}=\alpha_{n+1}\sigma_{n+1,n+1}=\alpha'_n\sigma_{nn}. \tag{2.58}$$

It is convenient to introduce the deviations from the bulk values

$$\alpha_{1n}\equiv\alpha_n-\alpha,\quad \alpha'_{1n}\equiv\alpha'_n-\alpha \tag{2.59}$$

and

$$b_{1n}\equiv b-b_n=\frac{d}{\eta}\left(\frac{1}{G}-\frac{1}{G^n}\right)=\frac{dG_{1n}}{\eta G G_n}, \tag{2.60}$$

where $\alpha$, $b$, and $G_{1n}$ are defined by Eq. (2.32), (2.6), and (2.12), respectively. The recurrence relations for the deviations $\alpha_{1n}$ and $\alpha'_{1n}$ have the form

$$\alpha_{1,n+1}=\frac{\alpha^2(2b_{1n}+\alpha_{1n})}{1-\alpha(2b_{1n}+\alpha_{1n})},\quad \alpha_{11}=-\alpha \tag{2.61}$$

and

$$\alpha'_{1,n-1}=\frac{\alpha^2(2b_{1n}+\alpha'_{1n})}{1-\alpha(2b_{1n}+\alpha'_{1n})},\quad \alpha'_{1,\infty}=0. \tag{2.62}$$

In terms of the deviations $\alpha_{1n}$, $\alpha'_{1n}$, and $b_{1n}$ the CF (2.53) can be now written as

$$\sigma_{nn}=\frac{d\theta}{\eta}\,\frac{1}{\sqrt{b^2-1}+\Sigma_n}, \tag{2.63}$$

where

$$\Sigma_n\equiv-(\alpha_{1n}+\alpha'_{1n})/2-b_{1n} \tag{2.64}$$

plays the role of the self-energy part for the spin CF. At and above $\theta_c$ the constraint equation (2.10) can be rewritten as

$$\int\frac{d^{d'}\mathbf{q}}{(2\pi)^{d'}}[\sigma_{nn}(\mathbf{q})-\sigma_{nn}^{\mathrm{bulk}}(\mathbf{q})]=0, \tag{2.65}$$

where the bulk result is given by Eq. (2.63) without $\Sigma_n$.

Since for $n\gg 1$ the quantities $\alpha_{1n}$ and $\alpha'_{1n}$ of Eq. (2.59) are small and $n$ in the recurrence relations (2.61) and (2.62) can be treated as a continuous variable, these relations can be reduced to the first-order nonlinear differential equations which for $\tilde{q}\equiv\sqrt{\kappa^2+q^2}\ll 1$ have the form

$$\frac{d}{dn}\alpha_{1n}=-2\tilde{q}\alpha_{1n}+\alpha_{1n}^2+2b_{1n},$$

$$-\frac{d}{dn}\alpha'_{1n}=-2\tilde{q}\alpha'_{1n}+(\alpha'_{1n})^2+2b_{1n}. \tag{2.66}$$

These Riccati equations can be transformed to linear second-order differential equations which are equivalent to Eq. (2.11).

### E. Variation of the gap parameter at low and high temperatures

The main problem with the solution of the ASM equations (2.5)–(2.10) is to find the variation of the gap parameter $G_n$ that plays a fundamental role in the theory. Its inhomogeneous part $G_{1n}$ defined by Eq. (2.12) is analogouos, as we shall see, to the function $V(z)$ with the opposite sign, which was considered by Bray and Moore [48]. The inhomogeneity $G_{1n}$ results from the deficit of interacting neighbors in the region near the surface and is positive. The simplest case in which $G_n$ can be found analytically is $T=0$. Here, for the magnetization one has $m_n=1$ everywhere, and $G_n$ determined from Eq. (2.8) reads

$$G_n=\begin{cases}\dfrac{2d}{2d-1}, & n=1\\ 1, & n\geqslant 2.\end{cases} \tag{2.67}$$

This result also shows that the boundary layer, $n=1$, is distinguished from all other ones. This feature that is beyond the scope of the continuous field-theoretical approaches can be observed in the whole temperature range. In particular, at high temperatures ($\theta\gg 1$), or in the whole region $\theta\geqslant\theta_c$ in the ''quasi-Ising'' limit $\eta\ll 1$, the variation of $G_n$ can be found with the help of the high-temperature series expansions (HTSE). This can be most conveniently done using the diagram technique for classical spin systems [49–51,33]. The result for the hypercubic lattice has the form ($\eta/\theta\ll 1$)

$$G_{1n}\cong\begin{cases}\dfrac{1}{\theta}\left(\dfrac{\eta}{2d\theta}\right)^2, & n=1\\ \dfrac{4(d-1)}{\theta}\left(\dfrac{\eta}{2d\theta}\right)^{2(n+1)}, & n\geqslant 2.\end{cases} \tag{2.68}$$

The terms with $n\geqslant 2$ are slightly different for the continuous-dimension model. One can see, again, that the

boundary layer is distinguished. For the layers with $n \geqslant 2$ the expected leading diagrams of order $2n$ are cancelled, and the result is much smaller.

Calculation of $G_{1n}$ in other cases requires more specialized methods, which will be considered below.

## III. SURFACE-INDUCED CORRELATIONS IN LOW AND HIGH DIMENSIONS

### A. Solution for the "toy" model $d=1$

In one dimension the solution of the ASM equations (2.5)–(2.10) is greatly simplified, since $d'=0$ and there is no integration over the wave vector $\mathbf{q}$. The quantity $b_n$ of Eq. (2.6) reduces in this case to $b_n = 1/(\eta G_n)$. For the autocorrelator $s_{nn}$ one has simply $s_{nn}=\sigma_{nn}$. Above $\theta_c$ the constraint equation (2.10) becomes $\sigma_{nn}=1$, i.e., all $\sigma_{nn}$ are equal to each other. This means that for the one-dimensional ASM the *transverse* susceptibilities with respect to the layer field, $\chi_{\perp nn}=\sigma_{nn}/\theta = 1/\theta$, are the same for all layers. Now, from the relation (2.58) follows $\alpha_{n+1}=\alpha_n'$. Using the latter together with the recurrence relations (2.54), one can write the constraint equation as

$$1=\sigma_{nn}=\frac{2\theta}{\eta}\begin{cases} 1/[2b_1-(2b_1)^{-1}], & n=1 \\ 1/[\alpha_n^{-1}-\alpha_n], & n\geqslant 2. \end{cases} \tag{3.1}$$

This implies that all $\alpha_n$ and $\alpha_n'$, except for $\alpha_1=0$, are equal to

$$\alpha=[\sqrt{\eta^2+\theta^2}-\theta]/\eta, \tag{3.2}$$

which is the bulk value given by Eq. (2.32). Then for $n\geqslant 2$ with the help of Eq. (2.32) one can identify $b_n=b=[\alpha+\alpha^{-1}]/2=\sqrt{\eta^2+\theta^2}/\eta$ and $\sqrt{b^2-1}=\theta/\eta$. The boundary-layer quantity $b_1$ can be determined directly from Eq. (3.1) with the result $2b_1=\alpha^{-1}=[\sqrt{\eta^2+\theta^2}+\theta]/\eta$. Now the exact result for $G_n=1/(\eta b_n)$ can be written in the form

$$G_n=\begin{cases} 2/[\sqrt{1+\theta^2-\theta_c^2}+\theta], & n=1 \\ 1/\sqrt{1+\theta^2-\theta_c^2}, & n\geqslant 2. \end{cases} \tag{3.3}$$

with $\theta_c=\sqrt{1-\eta^2}$. One can see that $G_1>G_{n\geqslant 2}=G$. In particular, in the weakly anisotropic case, $1-\eta \ll 1$, at criticality one has $G_1 \cong 2(1-\kappa)$, which is nearly two times greater than the bulk value $G=1$ [cf. Eq. (2.67)]. Variation of $G_n$ above belongs to the class studied at the end of Sec. II A, and thus $\sigma_{nn'}$ is given by Eq. (2.13). In our one-dimensional model, however, one has $\alpha-2b_{11}=0$, and the inhomogeneous term vanishes. Thus one arrives again at the result $\sigma_{nn}=1$, which can serve as an independent check of the calculations.

Now we consider the longitudinal CF $\sigma_{nn'}^{zz}$ and the corresponding susceptibilities. The solution of the finite-difference equation (2.5) with $\eta=1$ and $G_n$ given by Eq. (3.3) has the form (2.13) with $\alpha_z^{\pm 1}=b_z \mp \sqrt{b_z^2-1}$ [cf. Eq. (2.32)], $b_z \equiv 1/G$, and $b_{z11}\equiv 1/G-1/G_1$ [cf. Eq. (2.60)]. Using Eq. (3.3) one can write, explicitly,

$$\alpha_z=\sqrt{1+\theta^2-\theta_c^2}-\sqrt{\theta^2-\theta_c^2},$$

$$\frac{\alpha_z-2b_{z11}}{\alpha_z^{-1}-2b_{z11}}=\frac{\theta-\sqrt{\theta^2-\theta_c^2}}{\theta+\sqrt{\theta^2-\theta_c^2}}. \tag{3.4}$$

In contrast to the transverse CF $\sigma_{nn}$ given by Eq. (2.13), the inhomogeneous term in $\sigma_{nn}^{zz}$ does not disappear. For the weakly anisotropic ASM in the range $\theta \ll 1$, the expression for $\sigma_{nn}^{zz}$ simplifies to

$$\sigma_{nn}^{zz} \cong \frac{\theta}{\kappa_z}\left[1+\frac{\kappa_z-\kappa}{\kappa_z+\kappa}e^{-2\kappa_z(n-1)}\right] \tag{3.5}$$

[cf. Eq. (2.16)] where $\kappa$ and $\kappa_z$ are given by

$$\kappa \cong \theta, \quad \kappa_z \cong \sqrt{\theta^2-\theta_c^2}. \tag{3.6}$$

One can see that here the extrapolation length $\lambda_e=1/\kappa \gg 1$ is large on the scale of the lattice spacing. Well above $\theta_c$, where $\kappa_z \cong \kappa$, there is no difference between the longitudinal and transverse CFs: $\sigma_{nn}^{zz} \cong \sigma_{nn}=1$. Near $\theta_c$ one has $\kappa_z \ll \kappa$, and Eq. (3.5) shows the dependence on the distance from the surface. Whereas the bulk CF ($n=\infty$) diverges with the exponent $\gamma_{nn}^{\text{bulk}}=\frac{1}{2}$ (see the end of Sec. II C), the semi-infinite CF (3.5) does not for any finite $n$. In the boundary layer, $\sigma_{nn}^{zz}$ takes on the exact form

$$\sigma_{11}^{zz}=\frac{2\theta}{\theta+\sqrt{\theta^2-\theta_c^2}} \tag{3.7}$$

in the whole range of $\eta$. It varies from 1 at $\theta \gg \theta_c$ to 2 at $\theta \cong \theta_c$. At criticality the longitudinal surface susceptibility is two times greater than the transverse one. One can see that $\gamma_{11}=-1/2$, as in the MFA.

### B. Low dimensions, $1 \leqslant d \leqslant 2$

For $d>1$ the ASM equations become nontrivial because of the integration over the wave vector $\mathbf{q}$ in the constraint equations (2.10). The deviation $G_{1n}$ of the gap parameter from its bulk value is now nonzero for all layers, $n<\infty$. For $\theta \ll 1$, the system is close to criticality, and the inverse transverse correlation length $\kappa$ of Eq. (2.34) is small and related to $\theta$ by

$$\theta \cong 1/P \cong \kappa^{2-d}/C_d \tag{3.8}$$

[see Eqs. (2.27) and (2.39), cf. Eq. (3.6)]. The variation of $G_n$ is for $1 \leqslant d \leqslant 2$ close to that for the one-dimensional model above [see Eq. (3.3)] and can be searched in the form

$$G_n=\begin{cases} \dfrac{2d}{2d-1}G+\left(\dfrac{2d}{2d-1}\right)^2 G_{11}, & n=1 \\ G+G_{1n}, & n\geqslant 2. \end{cases} \tag{3.9}$$

The correction terms $G_{1n}$ will be shown below to be proportional to $(d-1)\theta$. [Note that the definition of $G_{11}$ here differs from that of Eq. (2.12).]

For the variation of the gap parameter above, the spin CF $\sigma_{nn}$ is for not too small wave vectors determined by the

boundary condition at the surface and given to the zeroth order by Eq. (2.15). This makes it possible to find $G_{1n}$ perturbatively in the range $\kappa n \ll 1$. After that one can study the corresponding corrections to $\sigma_{nn}$, which prove to be small for $q \gg \kappa$ or $d$ close to 1.

#### 1. Variation of $G_n$

The quantities $G_{1n}$ for $n \geq 2$ can be found from the constraint equation (2.10) written in the form $(d'/\Lambda^{d'}) \int dq q^{d'-1} \hat{\Delta}^2 \sigma_{nn} = 0$, where

$$\hat{\Delta}^2 \sigma_{nn} \equiv \sigma_{n+1,n+1} - 2\sigma_{nn} + \sigma_{n-1,n-1}. \tag{3.10}$$

The second-order difference above can, with the help of Eq. (2.58), be rewritten as

$$\hat{\Delta}^2 \sigma_{nn} = 2[-2\alpha b_{1n} + (\sqrt{b^2-1} - b_{1n}) \times (\alpha_{1n} + \alpha'_{1n}) - \alpha_{1n}\alpha'_{1n}]\sigma_{nn}. \tag{3.11}$$

Here the first term is the only one that is important in the long-wavelength region, $q \sim \kappa$. By integrating it one can set $\alpha \to 1$, which yields simply $-4b_{1n} \cong -4dG_{1n}$ in the constraint equation. All other terms make a contribution from $q \gg \kappa$, and the only important one among them is the term containing $(b^2-1)^{1/2}\alpha_{1n}$ where $\alpha_{1n}$ is induced by the surface. The latter can be found by comparing Eq. (2.15) with Eq. (2.63), where the small terms $\alpha'_{1n}$ and $b_{1n}$ are neglected. This results in

$$\alpha_{1n} \cong \frac{2(b^2-1)^{1/2}\alpha^{2n-1}}{1+\alpha^{2n-1}} \cong \frac{2\tilde{q}}{\exp(2\tilde{q}n)+1}, \tag{3.12}$$

where the second form is valid for $q \ll 1$. Using Eq. (2.15) for $q \gg \kappa$, one finally obtains

$$G_{1n} \cong \frac{\theta}{2}\frac{d'}{\Lambda^{d'}} \int_0^\Lambda dq q^{d'-1}(1-\alpha^2)\alpha^{2(n-1)}, \tag{3.13}$$

where the relation $2\alpha\sqrt{b^2-1} = 1-\alpha^2$ has been employed. This expression is explicitly small for $\theta \sim \kappa^{2-d} \ll 1$ or for $d' \equiv d-1 \ll 1$, as was said above. For $n \sim 1$, integration in Eq. (3.13) extends over the whole Brillouin zone, and $G_{1n}$ is nonuniversal. It decreases with $n$ since $\alpha < 1$. In the range $1 \ll n \ll 1/\kappa$ the integration is cut at $q \sim 1/n$, and one can use $\sqrt{b^2-1} \cong q$ and $\alpha^{2(n-1)} \cong e^{-2qn}$. Expression (3.13) then simplifies to

$$G_{1n} \cong \frac{d'}{\Lambda^{d'}}\frac{\theta\Gamma(d)}{(2n)^d} = \frac{\Gamma(d)}{dM_d}\frac{\kappa^{2-d}}{(2n)^d}, \tag{3.14}$$

where the second form is explicitly universal. Here $M_d$ is given by Eq. (2.41), or, near $d=2$, by Eq. (2.43). In two dimensions the result above regularizes to

$$G_{1n} \cong \frac{1}{8n^2 \ln[1/(a\kappa)]}, \tag{3.15}$$

where $a \sim 1$ is a nonuniversal factor. For $d > 2$ the values of $G_{1n}$ are no longer small, and the method used above fails. At distances $\kappa n \gtrsim 1$ the integral in Eq. (3.13) is dominated by $q \lesssim \kappa$, where $\sigma_{nn}$ and $\alpha_{1n}$ no longer have the forms (2.15) and (3.12). One can write $G_{1n}$ in the whole range of $\kappa n$ in the form

$$G_{1n} \cong \frac{\Gamma(d)}{dM_d}\frac{\kappa^2 g(\kappa n)}{(2\kappa n)^d}, \tag{3.16}$$

where $g(\kappa n)$ is a crossover function. The expected asymptote of $G_{1n}$ for $\kappa n \gg 1$ is

$$G_{1n} \sim \frac{\kappa^2}{(\kappa n)^\zeta} e^{-2\kappa n}, \tag{3.17}$$

with some exponent $\zeta$. The analytical calculation of the prefactor here seems to be very difficult.

The value of $G_{11}$ is fixed by the constraint equation (2.10) in the first layer. We will see below that $\Sigma_{n=1}^\infty G_{1n} \sim \kappa \ll \kappa^{2-d}$, thus $G_{11}$ is simply given by

$$G_{11} \cong -\sum_{n=2}^\infty G_{1n} \cong -\frac{\theta}{2}\frac{d'}{\Lambda^{d'}}\int_0^\Lambda dq q^{d'-1}\alpha^2, \tag{3.18}$$

where Eq. (3.13) has been used. Although the derivation above becomes invalid for $d$ close to 1, the resulting expression has a well defined form $G_{11} = -\kappa^{2-d}/2$ in this region, which will be confirmed below by another method and is in accord with the result $G_1 \cong 2(1-\kappa)$ in one dimension [see the discussion below Eq. (3.3)].

#### 2. Correlation functions near the surface

In low dimensions the quantities $G_{1n}$ are small, and one can try to find the corresponding corrections to the correlation functions perturbatively. It is clear, however, that since $G_{1n}$ can be responsible for the gap in the correlation function [see Eq. (2.16)] the direct perturbative approach to $\sigma_{nn}$ can be inefficient. It is more convenient to use perturbation theory with respect to the self-energy part $\Sigma_n$ in Eq. (2.63). For the variation of $G_n$ of the form (3.9) in the expression for the latter one has

$$b_{11} \cong \tfrac{1}{2} + dG_{11}$$
$$b_{1n} \cong dG_{1n}, \quad n \geq 2, \tag{3.19}$$

and the quantities $\alpha_{1n}$ and $\alpha'_{1n}$ can be found from the recurrence relations (2.61) and (2.62). These equations simplify, since $\alpha_{1n}$ for $n \geq 2$, as well as all $\alpha'_{1n}$, are induced by $G_{1n}$ and are small. For the first layer, taking into account $\alpha_{11} = -\alpha$ one obtains in the long-wavelength region

$$\sigma_{11} \cong \frac{2d\theta}{\tilde{q} + \Delta_1(\tilde{q}, \kappa)}, \tag{3.20}$$

where

$$\Delta_1(\tilde{q}, \kappa) \cong -2d\sum_{l=1}^\infty e^{-2\tilde{q}} G_{1l} \tag{3.21}$$

and the dependence of $\Delta_1$ on $\kappa$ is due to that of $G_{1n}$. The longitudinal CF $\sigma_{11}^{zz}$ is given by the same expressions with $\tilde{q}_z \equiv \sqrt{\kappa_z^2+q^2}$ instead of $\tilde{q} \equiv \sqrt{\kappa^2+q^2}$.

In the sum (3.21) only the term with $G_{11}$ is unknown, and its value follows from the constraint equation (2.65), which can, with the help of Eq. (2.38) and (2.39), be put into the form

$$\int_0^\Lambda dq q^{d'-1}\left[\frac{2}{\tilde{q}+\Delta_1(\tilde{q},\kappa)}-\frac{1}{\tilde{q}}\right]=0. \tag{3.22}$$

For $1<d<2$ the integral here is dominated by $q\sim\kappa$ and its upper limit can be set to $\infty$. This implies that $\Delta_1\sim\kappa$, i.e., the individual terms of the sum (3.21), each being of order $\theta \sim \kappa^{2-d} \gg \kappa$, are nearly cancelled. The ensuing expression for $G_{11}$ is given by Eq. (3.18) above.

As a result of the cancellation of the leading terms in Eq. (3.21), taking the next terms into account may become necessary. The $m$th-order terms in $G_{1n}$ are proportional to $\kappa^{m(2-d)}$ and they are small in comparison to $\kappa \ll 1$ for $d<2-1/m$. In particular, the first-order perturbation theory written above neglects the terms starting from $m=2$ and it is, in general, valid only for $d<1.5$. The second-order perturbation theory works for $d<1.75$, etc. The solution of the problem seems to undergo an infinite number of crossovers for $d$ approaching 2 and it should be rather complicated. Analytical solutions can be obtained for $d$ close to 1 and for $q \gg \kappa$, as well as in the marginal case $d=2$, with only logarithmic accuracy.

For $d' \equiv d-1 \ll 1$ one has $M_d \cong 1/(d-1)$, and the main contribution to the integral in Eq. (3.22) stems from the region $q \ll \kappa$. For $d=1$ the obvious solution of Eq. (3.22) is $\Delta_1(\kappa,\kappa)=\kappa$. Since for $d=1$ all $G_{1n}$ with $n\geqslant 2$ disappear, this leads to the one-dimensional result $G_{11}=-\kappa/2$. In the first order in $d-1$ one can still neglect the $q$ dependence of $\Delta_1(\tilde{q},\kappa)$. Then the perturbative solution of Eq. (3.22) leads to the simple result

$$\Delta_1(\kappa,\kappa)\cong d\kappa, \quad d-1\ll 1. \tag{3.23}$$

On the other hand, the sum (3.21) near $d=1$ consists of two contributions:

$$\Delta_1(\kappa,\kappa)\cong -2dG_{11}-\frac{\kappa^{2-d}}{M_d}\sum_{l=1}^{1/\kappa}\frac{1}{l^d}$$

$$\cong -2dG_{11}-\kappa^{2-d}(1-\kappa^{d-1}), \tag{3.24}$$

with logarithmic accuracy. Comparing it with Eq. (3.23) yields

$$G_{11}\cong -\frac{\kappa^{2-d}}{2}\cong -\frac{\kappa}{2}\left[1+(d-1)\ln\frac{1}{\kappa}\right]. \tag{3.25}$$

For the analysis of the limit $q\gg\kappa$ and of the behavior of the longitudinal CF $\sigma_{nn}^{zz}$ for small wave vectors, it is convenient to represent the quantity $\Delta_1(\tilde{q},\kappa)$ above as

$$\Delta_1(\tilde{q},\kappa)=\Delta_1(0,\kappa)+\overline{\Delta}_1(\tilde{q},\kappa), \tag{3.26}$$

where

$$\Delta_1(0,\kappa)\equiv -2d\sum_{l=1}^{\infty} G_{1l}$$

$$\overline{\Delta}_1(\tilde{q},\kappa)\equiv 2d\sum_{l=1}^{\infty}(1-e^{-2\tilde{q}l})G_{1l}. \tag{3.27}$$

The quantity $\Delta_1(0,\kappa)$ determines the gap of $\sigma_{nn}^{zz}$ at criticality ($\tilde{q}_z=0$) and it is related to $\Delta_1(\kappa,\kappa)$ studied above by

$$\Delta_1(0,\kappa)=\Delta_1(\kappa,\kappa)-2d\sum_{l=1}^{\infty}(1-e^{-2\kappa l})G_{1l}$$

$$\cong \Delta_1(\kappa,\kappa)-\frac{\kappa\Gamma(d)}{2^{d-1}M_d}\int_0^\infty\frac{dx}{x^d}(1-e^{-2x})g(x), \tag{3.28}$$

where the function $g(\kappa n)$ was introduced in Eq. (3.16). The integral term in this formula stems from the region $x\equiv\kappa n \sim 1$ where $g(\kappa n)$ is unknown. Even near $d=1$, where $\Delta_1(\kappa,\kappa)$ is given by Eq. (3.23) to the first order in $d-1$, calculation of this term needed to find $\Delta_1(0,\kappa)$ would require additional efforts. In general, there is no apparent way to calculate analytically the gap in $\sigma_{nn}^{zz}$. On the other hand, the existence of this gap can be anticipated, since the anisotropic model shows the mean-field critical behavior in all cases. At criticality for $q\ll 1$ the longitudinal CF can, after the expansion of Eq. (3.27), be written in the form

$$\sigma_{nn}^{zz}\cong\frac{2d\theta}{\Delta_1(0,\kappa)+Aq}, \tag{3.29}$$

where the stiffness of the longitudinal spin fluctuations is given by

$$A\cong 1+\frac{2^{2-d}\Gamma(d)}{M_d}\int_\kappa^\infty\frac{dx}{x^{d-1}}g(x), \tag{3.30}$$

which is again determined by the region $\kappa n\sim 1$, in general. For $d<2$ the lower limit of integration can be set to zero, and $A$ is a number. For $d\to 1$ the quantity $M_d$ diverges, and $A$ tends to 1. For $d\to 2$ the integral in Eq. (3.30) diverges logarithmically at the lower limit, and this divergence compensates that of $M_d$ [see Eq. (2.43)]. As a result, one obtains $A\cong 2+O[1/\ln(1/\kappa)]$. It should be stressed, however, that in fact $A$ cannot be calculated perturbatively, as above, if $d$ is not close to 1. This is because the term of the first-order in $G_{1n}$ gives a contribution comparable to the zeroth-order result, and so do the terms of all orders in $G_{1n}$.

The analytically tractable case is $q\gg\kappa$, in which the sum in Eq. (3.27) is dominated by $l\sim 1/q\ll 1/\kappa$ and one can use Eq. (3.14) for $G_{1n}$. Replacing this sum by the integral and combining it with Eq. (2.41) yields the result

$$\overline{\Delta}_1(q,\kappa)\cong\frac{\Gamma\left(\frac{d}{2}\right)\Gamma\left(\frac{3-d}{2}\right)}{\pi^{1/2}}\frac{1-q^{2-d}}{1-\kappa^{2-d}}(1-\kappa^{d-1})q\left(\frac{\kappa}{q}\right)^{2-d}. \tag{3.31}$$

Here the factor $1-q^{2-d}$ reflects the logarithmic divergence of the integral at the lower limit for $d$ close to 2, its counterpart $1-\kappa^{2-d}$ comes from $M_d$, and the factor $1-\kappa^{d-1}$ is due to the logarithmic divergence of the integral at the upper limit for $d$ close to 1. For $d$ not close to 1 or 2 these factors can be dropped. For $d=2$ the expression above regularizes to

$$\overline{\Delta}_1(q,\kappa)\cong q\ \ln(1/q)/\ln(1/\kappa) \tag{3.32}$$

with logarithmic accuracy. One can see that the $q$-dependent term calculated above is smaller than the leading term $q$ in the denominator of Eq. (3.20) by a factor $(\kappa/q)^{2-d}\ll 1$, which justifies using the perturbation theory in $G_{1n}$. This term depends on $\kappa$ and thus signifies the gap in the correlation function. For $2-d\ll 1$, the latter has a long-tail character, which makes the perturbation scheme slowly convergent. This is in contrast to the bulk behavior, where this gap tail stems simply from the expansion of $\tilde{q}=\sqrt{\kappa^2+q^2}$ and has the fast-decaying form $q(\kappa/q)^2/2$. The most drastic situation is realized for $d=2$, where the gap tail is logarithmic and the applicability of the perturbation theory requires fulfillment of the very difficult criterium $\ln(1/q)\ll\ln(1/\kappa)$.

One can improve the perturbation theory by taking into account the terms of the second order in $G_{1n}$ in the denominator of Eq. (3.20). These terms have the form of double sums over the layers and for $q\gg\kappa$ they make a contribution of order $q(\kappa/q)^{2(2-d)}$ to $\overline{\Delta}_1(q,\kappa)$. For $d=2$ the formulas simplify and one obtains the contribution $qR^2/2$, where $R$ is the ratio of logarithms in Eq. (3.32). In fact, in two dimensions one can sum up (with logarithmic accuracy) all orders of the perturbation theory in $G_{1n}$. This is possible because Eq. (2.11) with $G_{1n}$ given by Eq. (3.15) can be exactly solved in terms of the modified Bessel functions. The corresponding calculation will be presented below; here we discuss some further features of the semi-infinite ASM for $d\leqslant 2$.

In *each order* of the perturbation theory, $\Delta_1(q,\kappa)$ can be represented in the form (3.26), where $\overline{\Delta}_1(q,\kappa)$ is determined by $l\sim 1/\tilde{q}\gg 1$ and is thus universal. The quantity $\Delta_1(0,\kappa)$ is fixed by the constraint condition (3.22), where $q\sim\kappa\ll 1$, and it is thus universal, too. The same can be shown for all values of $n$, i.e., the spin CFs in the semi-infinite weakly-anisotropic ASM are universal in the whole half-space for $d<2$. In other words, in this case the *strong scaling* is realized, which manifests itself in the independence of the CFs of the lattice spacing $a_0$. Alternatively, this can be seen from the fact that the Green function equation (2.11) with the boundary condition (2.17) is applicable everywhere, because $G_{1n}$ are small and $\sigma_{nn'}$ is a smooth function of $n$ in the long wavelength region. The nonuniversality of $G_{1n}$ in several boundary layers does not play a role because $\sigma_{nn'}$ is sensitive only to the cumulative action of $G_{1n}$ from a large number of remote layers, $n\sim 1/\tilde{q}\gg 1$. For $d=2$ there are nonuniversal *logarithmic* corrections to the strong scaling. For $d>2$, as we shall see, the scaling is realized only in the asymptotic region $n\gg 1$.

The expressions for all $\sigma_{nn}$ can be obtained recurrently from $\sigma_{11}$ with the help of relation (2.58), which results in

$$\sigma_{nn}=\frac{\alpha'_{n-1}\alpha'_{n-2}\ldots\alpha'_1}{\alpha_n\alpha_{n-1}\ldots\alpha_2}\sigma_{11}. \tag{3.33}$$

Here, for $q\sim\kappa$ all $\alpha_n$ and $\alpha'_n$, except for $\alpha_1=0$, are close to unity. Thus all CFs in the layers near the surface are close to each other. At large distances the spin CFs should cross over to the bulk result (2.33) [cf. Eq. (3.5)]. For $q\sim\kappa$, this crossover occurs at $\kappa n\sim 1$ and it cannot be described analytically, since the solution depends on the values of $G_{1n}$ in this region, which have not been determined. For the wave vectors $q\gg\kappa$ the equation for $\sigma_{nn}$ can be solved perturbatively in $G_{1n}$ for all distances. This can be seen if one rewrites Eq. (2.11) in terms of the dimensionless variable $z\equiv qn$ and uses Eq. (3.14) for $G_{1n}$. Then the term with $G_{1n}$ in the equation becomes of order $(\kappa/q)^{2-d}/z^d$ and can be considered perturbatively for $d<2$. The solution is given (2.16) with $\tilde{q}\gg c$ plus a correction term. Near the surface, $z\equiv qn\ll 1$, to the lowest order in $z$ this solution can be put into the form (3.20) with $\Delta_n(\tilde{q},\kappa)\cong\overline{\Delta}_1(\tilde{q},\kappa)$ given by Eq. (3.31). For $z\equiv qn\gg 1$ one obtains

$$\sigma_{nn}\cong\frac{d\theta}{q}\left[1+\frac{\Gamma(d)}{2^d M_d}\left(\frac{\kappa}{q}\right)^2\frac{1}{(\kappa n)^d}\right], \tag{3.34}$$

which is in fact the expansion of $\sigma_{nn}\cong d\theta/\sqrt{\tilde{q}^2-2dG_{1n}}$ for large $q$. The latter result has a simple interpretation: For $q\gg 1/n\gg\kappa$ the surface term in $\sigma_{nn}$ is negligible, and the correction to the bulk result is due to $G_{1n}$ from the narrow region $|n''-n|\ll 1/q$, where $G_{1n}$ does not change significantly (the local correction).

For the longitudinal CF $\sigma^{zz}_{nn'}$, the corresponding effective wave vector $\tilde{q}_z\equiv\sqrt{\kappa_z^2+q^2}$ can be smaller than $\kappa$, especially at criticality, where $\tilde{q}_z=q$. For $\tilde{q}_z\ll\kappa$ the exponential decrease of $G_{1n}$ for $\kappa n\gtrsim 1$ [see Eq. (3.17)] comes into play. As a result, in the range $n\gtrsim n^*\sim 1/\kappa$ the free solution (2.16) is realized again. The disappearance of $G_{1n}$ for $n\sim 1/\kappa$ and the ensuing free solution is also characteristic for dimensions $2<d<4$. As we shall see below, for $d>4$ the value of $n^*$ is of the order of the lattice spacing, and the free solution is realized in a wider range. In contrast to the case $q\gg\kappa$ considered above, here the sign of the surface term in $\sigma^{zz}_{nn'}$ is negative. One can argue, in general, that the form of the free solution in the region $n^*\lesssim n\lesssim 1/\tilde{q}_z$ is Eq. (2.16) with a coefficient $f(\tilde{q}_z/\kappa)$ in front of the surface-induced term. The plausible assumption about the form of $f$ is $f=(\tilde{q}_z-c_{\rm eff})/(\tilde{q}_z+c_{\rm eff})$, i.e., the surface term of the CF changes sign as a function of the wave vector. As a justification one can stress that from the distances $n\gg n^*$ the region $n\lesssim n^*$, where the form of the CF is complicated, is seen as narrow. Thus one can replace this region with an effective boundary condition of the type (2.17) set at $n\sim n^*$. The quantity $c_{\rm eff}$ can be expected to be of order $\kappa$ in dimensions low enough. This is the exact result for $d=1$ [see Eq. (3.5)] and it will be shown numerically to hold for $d\leqslant 4$. This implies that the extrapolation length $\lambda_e=1/c_{\rm eff}$ is of the order of the *transverse* correlation length $\xi_{c\alpha}$, which (although nondivergent) is much greater than the lattice spacing for the weakly anisotropic systems near criticality. The important implication of

the negative sign of the surface term in $\sigma^{zz}_{nn'}$ at small wave vectors is the gap in $\sigma^{zz}_{nn'}$ at any finite distances from the surface, even at criticality. It is clear, although difficult to prove rigorously, that the existence of this gap in the asymptotic region, where the free solution is realized, also entails the gap in $\sigma^{zz}_{nn'}$ near the surface.

#### *3. Correlation functions for d=2*

Dimension $d=2$ is the marginal one between $d<2$, where the characteristic wave vectors in the spin CFs are $q \sim \kappa$, and $d>2$, where $q\sim 1/n$ are important. The solution with logarithmic accuracy for $d=2$ can be obtained if these ranges are separated by many decades, i.e., $\ln(1/\kappa)\gg \ln n$. In fact, the solution (3.15) for $G_{1n}$ has been obtained under this very restrictive condition. With this form of $G_{1n}$, the Green function equation (2.11) can be solved exactly in terms of the modified Bessel functions. This will be shown in more detail in Sec. IV A, and the result has the form (4.2) with

$$\mu \cong \frac{1}{2}\left[-1+\frac{1}{\ln(1/\kappa)}\right]. \tag{3.35}$$

For $qn\ll 1$ the expression for $\sigma_{nn}$ simplifies to

$$\sigma_{nn}\cong \frac{2d\theta}{q}(qn)^{1/\ln(1/\kappa)} \tag{3.36}$$

[cf. Eq. (4.9)]. This can be represented in the form of type (3.20) with $\Delta_n = q[1-(qn)^{-1/\ln(1/\kappa)}]$. For not too small $q$ one can expand $\Delta_n$ in powers of $\ln[1/(qn)]/\ln(1/\kappa)$ to obtain the gap tail of the spin CF. In this way the first-order result (3.32) for $n=1$ and all other orders of the perturbation theory in $G_{1n}$ are recovered.

At small wave vectors $q$, solution for $\sigma_{nn}$ is determined by $G_{1n}$ at $\kappa n\sim 1$ where the latter are unknown and hence $\sigma_{nn}$ does not have the form above. In fact, here the gap $\Delta_n(0,\kappa)$ in $\sigma_{nn}$ manifests itself, and it turns out to be much larger than the bulk gap $\kappa$. The dependence of $\Delta_n(0,\kappa)$ can be obtained from the constraint equation (2.65), where (3.36) and (2.33) are used and the integration over $q$ is performed between $\Delta_n(0,\kappa)$ and $1/n$. In this way one comes to an interesting formula:

$$\Delta_n(0,\kappa)\sim \kappa^{\ln 2}/n, \quad \ln n \ll \ln(1/\kappa). \tag{3.37}$$

Here the critical index ln2 results from the fact that $\sigma_{nn}$ of Eq. (3.36) is about 2 times greater than in the bulk; thus the gap in this region should be correspondingly greater to satisfy the constraint equation. The coefficient in Eq. (3.37) cannot be determined in the logarithmic aproximation; it should become universal for $n\gg 1$. This method is rather rough and it cannot distinguish detween the transverse and longitudinal correlation functions. One can expect that they differ by a numerical factor, as was confirmed by numerical calculations, which have been done, however, in a range of $\kappa$ not small enough to confirm formula (3.37) itself.

### C. High dimensions, $d\geqslant 4$

As we have seen above, for the weakly anisotropic ASM in low dimensions the problem can be solved analytically for $\kappa n\ll 1$ due to the separation of the $q$ ranges in the transverse CF $\sigma_{nn}$, as exemplified by Eq. (3.11). The surface-induced term is important for $q\sim 1/n\gg\kappa$, whereas the term induced by $G_{1n}$ dominates for $q\sim\kappa\ll 1$. In high dimensions the separation of the $q$ ranges of both terms also takes place, although in a different form. Whereas the $q$ range of the surface term remains $q\sim 1/n$ (for $\kappa n\ll 1$), the $G_{1n}$-induced term dominates in the range $q\sim 1$. Thus the ranges separate at distances $n\gg 1$, where the problem can be solved analytically. Henceforce in this subsection we will consider the close-to-criticality case $\kappa\ll 1$; otherwise, at distances $n\gg 1$ deviations from the bulk values will be too small [cf. Eq. (2.68)].

The surface term of $\sigma_{nn}$ has in high dimensions the opposite sign, as compared to the low-dimensional result (2.15), and for $n\gg 1$ its form does not depend on the details of the behavior in the region close to the surface. As we will see below, for $d\geqslant 4$ the quantity $G_{1n}$ decays fast with $n$, and for the calculation of the surface term it can be neglected starting from some $n^*\gg 1$. For $n\geqslant n^*$ one can use for $\sigma_{nn'}$ an expression of the type (2.13), where $2b_{11}$ is replaced by some quantity determined by the region $n\leqslant n^*$. In contrast to the low-dimensional case, there is no reason for the substitute for $2b_{11}$ to be close to unity, because the variation of $G_n$ is no longer close to Eq. (3.9), or in Eq. (3.9) $G_{1n}$ are no longer small. At large distances and small wave vectors one can thus use Eq. (2.16) where the coefficient $f(q)$ in front of the surface term is close to $-1$, since the quantity $c_{\rm eff}$ should be of order unity (the extrapolation length $\lambda_e \equiv 1/c_{\rm eff}$ comparable to the lattice spacing).

Since postulating $\sigma_{nn'}$ in the form (2.16) is not quite a rigorous procedure, let us consider another derivation based on the continued-fraction formalism described in Sec. II D. For $n\gg 1$ one can employ the differential equations (2.66) for the quantities $\alpha_{1n}$ and $\alpha'_{1n}$ of Eq. (2.59). The boundary condition for the second equation is $\alpha'_{1\infty}=0$; the quantity $\alpha'_{1n}$ is generated solely by $G_{1n}$ and it is not related to the surface term of $\sigma_{nn}$. For the equation for $\alpha_{1n}$ the boundary condition cannot be set on the surface, since this equation is invalid for $n\sim 1$. Thus we use the boundary condition $\alpha_{1n}=\alpha_{1n*}$ at $n=n^*\gg 1$, where $\alpha_{1n*}$ is determined by the exact recurrence formula (2.61) in the region $n\leqslant n^*$. For $n>n^*$ one can neglect $2b_{1n}$ in the differential equation for $\alpha_{1n}$, after which it can be linearized with respect to the new variable $1/\alpha_{1n}$ and solved to give

$$\alpha_{1n}=\frac{2\tilde{q}\alpha_{1n*}}{\alpha_{1n*}+(2\tilde{q}-\alpha_{1n*})\exp[2\tilde{q}(n-n^*)]}. \tag{3.38}$$

Since $\alpha_{1n*}$ is generated by the boundary condition at the surface and by $b_{1n}$, which are not explicitly small for $n\leqslant n^*$, one has $|\alpha_{1n*}|\gg\tilde{q}$ for small wave vectors. It can be seen that $\alpha_{1n*}$ cannot be positive, otherwise $\alpha_{1n}$ turns to infinity at $n$ determined by $\exp[2\tilde{q}(n-n^*)]=\alpha_{1n*}/(\alpha_{1n*}-2\tilde{q})\cong 1$. Thus, $\alpha_{1n*}<0$, and in the relevant region $n\gg n^*$, $\tilde{q}n\sim 1$ (3.38) simplifies to the form

$$\alpha_{1n}\cong -\frac{2\tilde{q}}{\exp(2\tilde{q}n)-1}, \tag{3.39}$$

which is independent of the behavior in the boundary region, $n \leqslant n^*$. For $\tilde{q}n \sim 1$ one has $\alpha_{1n} \sim 1/n$; thus in the differential equation (2.66) $\tilde{q}\alpha_{1n} \sim \alpha_{1n}^2 \sim 1/n^2$. This implies that the method used here works if $G_{1n} \propto b_{1n}$ decays faster than $1/n^2$. As we shall see shortly, this is the case for $d \geqslant 4$. Now the surface term of $\sigma_{nn}$ can be found from Eqs. (2.63) and (2.64) with $\alpha'_{1n} = b_{1n} = 0$, which results in Eq. (2.16) with $f(q)$ close to $-1$.

For $q \sim 1$ and $n \gg 1$ the quantity $\alpha_{1n}$ of Eq. (3.39), as well as the surface term in Eq. (2.16), are exponentially small. Here the $G_{1n}$-induced term becomes dominant. To find the values of $\alpha_{1n}$ and $\alpha'_{1n}$ in this region, one can drop the small terms $\alpha_{1n}^2$ and $(\alpha'_{1n})^2$ in Eq. (2.66), after which the linear inhomogeneous differential equations can be solved. The solution at point $n$ is induced by $b_{1n''}$ from the interval of $n''$ around $n$, which satisfies $|n''-n| \sim 1/\tilde{q} \sim 1 \ll n$; thus one can treat $b_{1n}$ in Eq. (2.66) as a constant. The solution of Eq. (2.66) has the form $\alpha_{1n} \cong \alpha'_{1n} \cong \alpha b_{1n}/\sqrt{b^2-1}$, and the quantity $\Delta_n$ of Eq. (2.64) reads $\Delta_n \cong -b b_{1n}/\sqrt{b^2-1}$. The resulting correction to $\sigma_{nn}$ given by Eq. (2.63) is of the form

$$\delta\sigma_{nn}^{\text{local}} \cong d\theta \frac{b b_{1n}}{(b^2-1)^{3/2}} = -b_{1n} \frac{\partial}{\partial b} \sigma_{nn}^{\text{bulk}}, \qquad (3.40)$$

where $\sigma_{nn}^{\text{bulk}}$ is given by Eq. (2.32) or by the first term of Eq. (2.16). This correction is due to the local deviation of $b_n$ from the bulk value $b$ [see Eq. (2.60)] and it could in fact be written for $q \sim 1$ without calculations.

Now the value of $b_{1n}$ can be found from the constraint equation (2.65), where $\sigma_{nn}$ is the sum of Eqs. (2.16) and (3.40). One can see that $b_{1n} > 0$ is needed to compensate for the negative surface term. The integration of the local term (3.40) extends for $d > 4$ over the whole Brillouin zone, $q \sim 1$, and can be accomplished with the use of Eq. (2.38). This results in

$$\frac{d'}{\Lambda^{d'}} \int_0^{\Lambda} dq q^{d'-1} \frac{b b_{1n}}{(b^2-1)^{3/2}} = \frac{b_{1n}}{d^2} P(\eta G) I(\eta G), \qquad (3.41)$$

where $I(X)$ is defined by Eq. (2.45). Since for $d > 4$ both $P(X)$ and $I(X)$ do not diverge for $X \to 1$, one can set $X = 1$ for weakly anisotropic ASM near criticality. The integration of the surface term is cut at $q \sim 1/n \ll 1$ for $\kappa n \ll 1$ and at $q \sim q^* = \sqrt{\kappa/n}$ $(1/n \ll q^* \ll \kappa)$ for $\kappa n \gg 1$. The resulting $G_{1n} \cong b_{1n}/d$ has for $d > 4$ and $n \gg 1$ the form

$$G_{1n} \cong \frac{d'}{\Lambda^{d'}} \frac{d\Gamma[(d-1)/2]}{P(1)I(1)} \frac{\kappa^{d-2}}{(\kappa n)^{(d-2)/2}} K_{(d-2)/2}(2\kappa n), \qquad (3.42)$$

where $K_\nu(x)$ is the Macdonald (modified Bessel) function. For the hypercubic lattices the first fraction in Eq. (3.42) should be replaced according to Eq. (2.36) by $S_{d'}/(2\pi)^{d'}$ [see Eq. (2.40)]. One can see that the form of $G_{1n}$ is nonuniversal. The limiting forms of Eq. (3.42) are

$$G_{1n} \cong \frac{d'}{\Lambda^{d'}} \frac{d\Gamma(d-2)}{P(1)I(1)} \frac{1}{(2n)^{d-2}}, \quad \kappa n \ll 1, \qquad (3.43)$$

and

$$G_{1n} \cong \frac{d'}{\Lambda^{d'}} \frac{d\Gamma[(d-1)/2]}{2P(1)I(1)} \frac{\kappa^{d-2} e^{-2\kappa n}}{(\kappa n)^{(d-1)/2}}, \quad \kappa n \gg 1. \qquad (3.44)$$

If $d$ is close to the marginal value $d = 4$ the contribution to the integral (3.41) from small wave vectors becomes large, and separation of the $q$ ranges in $\sigma_{nn}$ no longer takes place. Nevertheless, the problem can be solved analytically with logarithmic accuracy at distances $\kappa n \ll 1$. In this case one should integrate in Eq. (3.41) down to $q \sim 1/n \gg \kappa$ where the surface term in Eq. (2.16) becomes important. This leads to the replacement

$$P(1)I(1) \Rightarrow \frac{d'}{\Lambda^{d'}} \frac{16}{d-4} \left[ 1 - \frac{1}{(an)^{d-4}} \right] \qquad (3.45)$$

in Eq. (3.43), $a$ being a lattice-dependent number. For $G_{1n}$ near $d = 4$ one obtains the result

$$G_{1n} \cong \frac{1}{16n^2} \frac{d-4}{(an)^{d-4}-1}, \qquad (3.46)$$

which regularizes to

$$G_{1n} \cong \frac{1}{16n^2 \ln(an)}, \quad 1 \ll n \ll 1/\kappa, \qquad (3.47)$$

in four dimensions.

It can be seen that the applicability condition of the method used here, $G_{1n} = o(1/n^2)$ for $n \gg 1$, is satisfied for $d \geqslant 4$. In the range $2 < d < 4$ an attempt to apply (for $\kappa = 0$) the same method yields for the integral (3.41) a value of order $\sim b_{1n} n^{4-d}$ that stems from the region $q \sim 1/n$. The integral of the inhomogeneous term in Eq. (2.16) is, for $\kappa = 0$, determined by the same range of $q$ and it is proportional to $n^{2-d}$. Equating both contributions according to Eq. (2.65) yields $G_{1n} \propto b_{1n} \propto 1/n^2$ with some universal coefficient. One can see that formula (3.46) shows such a behavior for $d < 4$ where the term containing the nonuniversal number $a$ is small. In fact, it joins smoothly the exact solution (4.1) for $2 < d < 4$ found by Bray and Moore [48], which will be considered in the next section.

The susceptibilities of the ASM in high dimensions show the mean-field critical behavior. In particular, at small wave vectors one can drop the local contribution (3.40) and use Eq. (2.16) for $\sigma_{nn}$ at distances far enough from the surface, $n \gtrsim n^*$. For $q = 0$ and $\kappa n, \kappa_z n \ll 1$ both transverse and longitudinal CFs [see Eq. (2.16)] simplify to (2.18). CFs in the surface region, $n \lesssim n^*$, should be calculated numerically. Since $\sigma_{11}$ can be obtained from the CFs $\sigma_{nn}$ far from the surface with the help of relation (3.33) and the quantities $\alpha_n$ and $\alpha'_n$ are nonsingular, $\sigma_{11}$ shows the same critical behavior as in the asymptotic region $n \gg 1$. The latter is characterized in particular by $\gamma_{11} = -\frac{1}{2}$, which can be found by expanding

Eq. (2.16) for $q=0$ up to the second order in $\tilde{q}=\kappa\ll 1$ and using $\kappa\propto\tau^{1/2}$ following from Eqs. (2.34) and (2.47).

Finally, let us transform the CF $\sigma_{nn'}(q)$ to the real-space CF $\sigma_{nn'}(\rho)$, where $\rho$ is the distance between two points in the direction parallel to the surface. At large distances, $n,n',\rho\gg 1$ the relevant values of $q$ are small and one can use Eq. (2.16) with $\tilde{q}=q\ll c$, disregarding the local contribution (3.40). The condition for this is $e^{qn}\ll(qn)^2n^{d-4}$, which is satisfied for $d>4$ and $n\gg 1$. Then one comes to the MFA result, which, at isotropic criticality, $\kappa=0$, has the form [5]

$$\sigma_{nn'}(\rho)\propto\left\{\frac{1}{[\rho^2+(n-n')^2]^{(d-2)/2}}-\frac{1}{[\rho^2+(n+n')^2]^{(d-2)/2}}\right\} \tag{3.48}$$

with a nonuniversal factor depending on the lattice structure. In this expression the surface-induced term with $n+n'$, which is similar to the ''image'' term in electrostatic problems, modifies its asymptotes at $\rho\gg n,n'$ and $n\gg\rho,n'$. These are [5,11]

$$\sigma_{nn'}(\rho)\propto 1/\rho^{d-2+\eta_\parallel},\quad \eta_\parallel=2 \tag{3.49}$$

for $n,n'=\text{const}$ and $\rho\gg n,n'$ and

$$\sigma_{nn'}(\rho)\propto 1/n^{d-2+\eta_\perp},\quad \eta_\perp=1 \tag{3.50}$$

for $\rho,n'=\text{const}$ and $n\gg\rho,n'$. One can see that near the surface correlations decay faster than in the bulk ($\eta_b=0$), especially in the direction parallel to the surface.

## IV. DIMENSIONS BETWEEN TWO AND FOUR

### A. Isotropic model at criticality

As we have seen above, in low and high dimensions the correlation function $\sigma_{nn}$ consists of two different (surface and local) terms, which are dominant in different ranges of $q$. This property makes possible an analytical solution of the problem for $\kappa n\ll 1$ in low dimensions and for $n\gg 1$ in high dimensions. In the range $2<d<4$ both terms are dominated by the range $q\sim 1/n$, i.e., they cannot be separated from each other. Fortunately, the problem has an exact solution for the isotropic model at criticality for $n\gg 1$ [48], where the anticipated asymptote of $G_{1n}$ far from the surface can be written as [see the discussion after Eq. (3.47)]

$$G_{1n}=\frac{\frac{1}{4}-\mu^2}{2dn^2},\quad \mu=\frac{d-3}{2}, \tag{4.1}$$

where the choice of the parameter $\mu$ will be justified below. For $n\gg 1$ and $q\ll 1$ one can use the second-order differential equation (2.11) for the transverse CF, in which $\tilde{q}=q$ at isotropic criticality. The latter can be solved in terms of the modified Bessel functions:

$$\sigma_{nn'}=2d\theta\begin{cases}\sqrt{nn'}I_\mu(qn)K_\mu(qn'), & n\leqslant n'\\ \sqrt{nn'}I_\mu(qn')K_\mu(qn), & n'\leqslant n,\end{cases} \tag{4.2}$$

where the term $C(nn')^{1/2}K_\mu(qn)K_\mu(qn')$ could also be added. This solution looks similar to the full discrete solution (2.50), but here the constant $C$ cannot be found from the boundary condition at the surface, since Eq. (2.11) is only valid for $n\gg 1$.

There is, however, another method of finding $\sigma_{nn'}$ [48] that avoids using the boundary condition at the surface and yields $C=0$. The consideration starts with the eigenvalue problem

$$\left(\frac{d^2}{dn^2}+\frac{\frac{1}{4}-\mu^2}{n^2}\right)\psi(a,n)=-a^2\psi(a,n), \tag{4.3}$$

whose solution $\psi(a,n)=\sqrt{an}J_\mu(an)$ satisfies

$$\int_0^\infty dn\ \psi(a,n)\psi(a',n)=\delta(a-a'),$$

$$\int_0^\infty da\ \psi(a,n)\psi(a,n')=\delta(n-n') \tag{4.4}$$

and thus forms an orthogonal and complete basis on the semi-infinite interval. Then the Green function $\sigma_{nn'}$ can be expressed through its decomposition over the set of eigenfunctions as

$$\sigma_{nn'}=2d\theta\int_0^\infty da\,\frac{\psi(a,n)\psi(a,n')}{a^2+q^2}, \tag{4.5}$$

which results in Eq. (4.2) without any additional terms.

Now the value of $\mu$ can be found from the constraint condition in the form (2.65) with the bulk CF given by Eq. (2.33), i.e.,

$$n\int_0^\infty dz\ z^{d-2}\left[2I_\mu(z)K_\mu(z)-\frac{1}{z}\right]=0. \tag{4.6}$$

This integral, which can be found in Ref. [48], is zero for all $n$ if $\mu$ is given by Eq. (4.1) and $2<d<4$. There is another solution, $\mu=(d-5)/2$ for $3<d<4$, which leads to negative values of $G_{1n}$ and it should be disregarded for the ordinary phase transition considered here. The asymptotic form of the layer autocorrelation function $\sigma_{nn}$ of (4.2) for $qn\gg 1$ is

$$\sigma_{nn}\cong\frac{d\theta}{q}\left[1+\frac{\frac{1}{4}-\mu^2}{2(qn)^2}\right]. \tag{4.7}$$

Here the first term is the bulk CF and the second term in the square brackets, $dG_{1n}/q^2$, is the local contribution analogous to that in Eq. (3.34). This form of $\sigma_{nn}$ is responsible for the convergence of the integral in Eq. (4.6) at $z\equiv qn\sim 1$, i.e., for $q\sim 1/n\ll 1$. The latter justifies using the long-wavelength approximation in the scaling region, $n\gg 1$. Here the discrete lattice structure does not show up in the long-wavelength behavior of $\sigma_{nn'}$ and in the form of $G_{1n}$, thus $1/n$ is the only scale for $q$. In the opposite limit, $qn\ll 1$, one can use

$$I_\mu(z)\cong\frac{1}{\Gamma(1+\mu)}\left(\frac{z}{2}\right)^\mu[1+O(z^2)],\quad z\ll 1$$

$$K_\mu(z)=\frac{\pi}{2\sin(\pi\mu)}[I_{-\mu}(z)-I_\mu(z)] \tag{4.8}$$

to express $\sigma_{nn}$ in the form

$$\sigma_{nn}\cong\frac{d\theta n}{\mu}\left[1-\frac{\Gamma(1-\mu)}{\Gamma(1+\mu)}\left(\frac{qn}{2}\right)^{2\mu}\right]. \tag{4.9}$$

For $d>3$ one has $\mu>0$ and $\sigma_{nn}$ does not diverge at $q\to 0$ for any finite $n$. Conversely, for $d<3$ one has $\mu<0$, and thus the second singular term in Eq. (4.9) is dominant and it causes the divergence of $\sigma_{nn}$ at small $q$. In the marginal case $d=3$, Eq. (4.9) regularizes to

$$\sigma_{nn}\cong 2d\theta n\left[\ln\frac{1}{qn}+c_0\right],\quad c_0=\ln 2-\gamma, \tag{4.10}$$

where $\gamma=0.5772\ldots$ is the Euler constant and $c_0\approx 0.1159$ is rather small.

The Fourier transformed CF (4.2) looks very beautiful in real space [48]:

$$\sigma_{nn'}(\rho)=\frac{2d\theta\Gamma(d-2)}{(4\pi)^{(d-1)/2}\Gamma[(d-1)/2]}\times\left[\frac{1}{\rho^2+(n-n')^2}-\frac{1}{\rho^2+(n+n')^2}\right]^{(d-2)/2}. \tag{4.11}$$

Here, in contrast to the MFA result (3.48), the bulk term and the surface-induced image term are *nonadditive*. The critical exponents $\eta_\parallel$ and $\eta_\perp$ determined analogously to Eq. (3.49) and (3.50) are $\eta_\parallel=d-2$ and $\eta_\perp=(d-2)/2$ [48].

In spite of the apparent similarity of the solution presented here and that of Bray and Moore [48], they are not completely identical. The difference is that in the spin vector model used here the constraint $|\mathbf{m}_i|=1$ on each lattice site is obeyed, which is accounted for in the constraint equation (2.4). Bray and Moore used the phenomenological $\phi^4$ field-theoretical model with the $O(\infty)$ symmetry, which has no constraint on the field $\phi$. Accordingly, the self-consistent determination of the function $V(z)$ [48], which is analogous to $-G_{1n}$ here, is more complicated and can be done only for the single $d$-dependent magic value of the coupling constant $u$.

A peculiar feature of the differential equation (2.11) is that its solution (4.2) is twofold: for a given $\mu^2$ in Eq. (4.1) solutions with both signs of $\mu=\pm|\mu|$ can be realized for $d>3$ and $d<3$. Accordingly, the eigenvalue problem (4.3) has two sets of eigenfunctions that form two different orthogonal and complete bases. An apparent reason for such a behavior is the singularity of $G_{1n}$ at $n=0$ in the continuous approach, which is, naturally, not present in the original discrete formulation of the problem. This singularity and the concomitant loss of the boundary condition at the surface could be circumvented by Bray and Moore by application of the eigenfunction trick above, which looks like a miracle (see other examples from quantum mechanics in Ref. [52]). However, the fact that the same differential equation has different solutions, e.g., for $d=2.5$ and $d=3.5$, contradicts common sense and, more importantly, impedes numerical solution of this equation. The latter would be the only possibility in situations where no general analytical solution is available, as in the off-criticality case; and in that case the loss of the boundary condition creates insurmountable difficulties.

The key to the paradox is that in the original discrete formulation there is no singularity of $G_{1n}$, and the values of $2dG_{1n}$ are *different* for $d>3$ and $d<3$, although they may coincide in the scaling region, $n\gg 1$. The (rather essential) difference between the CFs $\sigma_{nn'}$ for $d>3$ and $d<3$ stems entirely from the nonscaling region, $n\sim 1$, which is not amenable to the field-theoretical methods. This is most pronounced in the limits $d\to 2$ and $d\to 4$, where $G_{1n}$ of Eq. (4.1) tends to zero in the scaling region but $\sigma_{nn}$ of (4.2) remains well defined and given by

$$\sigma_{nn}\cong\frac{d\theta}{q}(1\pm e^{-2qn}),\quad d\to\begin{Bmatrix}2\\4\end{Bmatrix}. \tag{4.12}$$

The latter is nothing more than the particular forms of Eq. (2.16), the difference between the two expressions being *completely* determined by the nonscaling region near the surface. For $d\to 2$, the parameter $c$ in Eq. (2.16) disappears with $\kappa$ in the isotropic limit, and the coefficient in front of the surface terms is $f=1$. For $d\to 4$, the parameter $c$ is of order unity, and for $q\ll 1$ the surface term is negative, $f\cong -1$. Thus the isotropic-criticality solution of Bray and Moore smoothly joins the solutions obtained for $d\leqslant 2$ and $d\geqslant 4$.

To close this subsection let us look at how the continued-fraction formalism of Sec. II D works at isotropic criticality. Here $\sigma_{nn}$ is given by Eq. (2.63), where $\sqrt{b^2-1}\cong q$ in the long-wavelength region and $b_{1n}\cong dG_{1n}\sim 1/n^2$ can be neglected for $n\gg 1$. The quantities $\alpha_{1n}$ and $\alpha'_{1n}$ can be found from the first-order nonlinear differential equations (2.66) with $\tilde{q}=q$. The latter can be reduced to the second-order linear differential equations and solved to give

$$\alpha_{1n}=-\frac{d}{dn}\ln\{e^{-qn}\sqrt{qn}[I_\mu(qn)+CK_\mu(qn)]\},$$

$$\alpha'_{1n}=\frac{d}{dn}\ln\{e^{qn}\sqrt{qn}[K_\mu(qn)+C'I_\mu(qn)]\}. \tag{4.13}$$

Here the integration constant $C'$ should be set to zero, since $\alpha'_{1n}$ vanishes at infinity. The constant $C$ remains undefined due to the loss of the boundary condition at the surface for the equation for $\alpha_{1n}$. Adopting these results in Eq. (2.63) and using $I_\mu(z)K'_\mu(z)-I'_\mu(z)K_\mu(z)=-1/z$ leads to the previously obtained expression (4.2) for $n'=n$, with the same additional term containing $C$. Thus one should set $C=0$ in Eq. (4.13). Then from Eq. (4.8) it can be seen that $\alpha_{1n}$ is nonsingular at $qn\ll 1$ and the singular terms in $\sigma_{nn}$ [see Eq. (4.9)] are due solely to $\alpha'_{1n}$. Another way of obtaining Eq. (4.13) is to use the definitions (2.59) and (2.52) to identify $\mathcal{I}_n=\sqrt{n}I_\mu(qn)$ and $\mathcal{K}_n=\sqrt{n}K_\mu(qn)$. The limiting forms of $\alpha_{1n}$ and $\alpha'_{1n}$ are

$$\alpha_{1n}\cong\frac{1}{n}\times\begin{cases}-\frac{1}{2}-\mu, & qn\ll 1\\ \frac{\frac{1}{4}-\mu^2}{2qn}\left[1+\frac{1}{qn}\right], & qn\gg 1\end{cases}\tag{4.14}$$

and

$$\alpha'_{1n}\cong\frac{1}{n}\times\begin{cases}\frac{1}{2}-|\mu|, & qn\ll 1\\ \frac{\frac{1}{4}-\mu^2}{2qn}\left[1-\frac{1}{qn}\right], & qn\gg 1.\end{cases}\tag{4.15}$$

The results above will be used in the numerical solution of the semi-infinite ASM at the isotropic criticality.

### B. Away from anisotropic criticality

The transverse correlation function $\sigma_{nn'}$ behaves similarly for the isotropic model slightly above $\theta_c$ and for the weakly anisotropic model at or slightly above $\theta_c$. In both cases the behavior of $\sigma_{nn'}$ is modified in comparison to that at isotropic criticality due to the finiteness of the transverse correlation length $\xi_{c\alpha}=1/\kappa$, where $\kappa$ is given by Eq. (2.34). For $0<\kappa\ll 1$ the function $G_{1n}$ has in the scaling region $n\gg 1$ the form generalizing Eq. (4.1):

$$G_{1n}=\frac{\frac{1}{4}-\mu^2}{2dn^2}g(\kappa n).\tag{4.16}$$

For $\kappa n\gg 1$ one can expect, as is the case in other dimensions [see, e.g., Eq. (3.44)], $g(\kappa n)\propto e^{-2\kappa n}$ with some $n$-dependent prefactor. Analytical calculation of this prefactor seems to be impossible. In the opposite limit $g$ can be written in the form

$$g(\kappa n)\cong 1-a_d(\kappa n)^r,\quad \kappa n\ll 1,\tag{4.17}$$

with $r>0$ and $a_d\sim 1$. There is no guess about the concrete form of $g(\kappa n)$ in the intermediate region and, moreover, even if $g(\kappa n)$ is known, one would not be able to find a general analytical solution for the differential equation (2.11). For the field-theoretical model [48] the question of how to generalize the choice of the coupling constant $u$ for $\kappa\neq 0$ [be it the magic value $u^*(d)$ or something else] further complicates the problem and makes it quite intractable. For the ASM, however, the situation is not so hopeless: Some features of the off-criticality behavior can be studied analytically using available small parameters; its general properties are well described by the scaling, and the rest can be done numerically.

#### 1. Scaling form of correlation functions

It is convenient to start the consideration with the longitudinal correlation function $\sigma^{zz}_{nn'}$. The latter satisfies in the scaling region $n\gg 1$ Eq. (2.11) with $\tilde{q}^2\Rightarrow\kappa_z^2+q^2$ and $G_{1n}$ given by Eq. (4.16). In the generic case of the anisotropic criticality the longitudinal correlation length $\xi_{cz}$ goes to infinity and one has $\kappa_z\equiv 1/\xi_{cz}=0$ in Eq. (2.11). In this case, for $n=n'$ there are only three length parameters entering into the longitudinal CF: $n$, $1/q$, and the transverse correlation length $\xi_{c\alpha}\equiv 1/\kappa$. Thus $\sigma^{zz}_{nn}$ can be written at $\theta_c$ in the two-parameter scaling form

$$\sigma^{zz}_{nn,\theta_c}(\kappa,q)=\frac{d\theta}{\kappa}\Phi(x,y),\quad x\equiv\kappa n,\quad y\equiv\frac{q}{\kappa}.\tag{4.18}$$

Away from criticality one more length parameter, $\xi_{cz}$, appears, but it does not complicate the problem. As can be seen from Eq. (2.11), $\sigma^{zz}_{nn}(\kappa,\kappa_z,q)$ can be represented in the same form with $y\Rightarrow\sqrt{(\kappa_z/\kappa)^2+y^2}$. Similarly, the transverse CF $\sigma_{nn}(\kappa,q)$ is given by Eq. (4.18) with $y\Rightarrow\sqrt{1+y^2}$. For the isotropic model or above the anisotropic crossover temperature $\tau^*$ [see the discussion following Eq. (2.48)] the longitudinal CF coincides with the transverse CF.

It should be stressed that in the ASM the transverse correlation length plays the main role, whereas the longitudinal one, which does not enter into the ASM equations (2.5)–(2.10), is a subordinate quantity. This feature, which should be to some extent shared by the weakly anisotropic classical Heisenberg model, provides a contrast to the usual scaling scheme using the diverging $\xi_{cz}$ as the main scaling parameter (see, e.g., Refs. [11,12]).

Let us now study the limiting forms of the scaling function $\Phi(x,y)$. The bulk limit $\Phi^{\rm bulk}(x,y)=1/y$ is clearly realized for $z\equiv xy=qn\gg 1$. The isotropic criticality limit $\Phi^{\rm isocrit}(x,y)=2xI_\mu(xy)K_\mu(xy)$ studied above is achieved if $y\gg 1$ provided that $x\ll 1$. Both of these conditions imply that $1/\kappa$ becomes greater than other length scales. For $x\gg 1$ the quantities $G_{1n}$ become exponentially small, and in the long-wavelength region $\sigma^{zz}_{nn,\theta_c}$ is given by Eq. (2.16), as in high dimensions. This implies the scaling function

$$\Phi^{x\gg 1}(x,y)\cong[1-e^{-2(x+x_e)y}]/y,\tag{4.19}$$

where $x_e\equiv\kappa\lambda_e\sim 1$ is the scaled extrapolation length. This expression could also be written in the form of the type (2.16), which makes no difference in the relevant region $y\ll 1$. One can see that the longitudinal CF at criticality does not diverge for $q\to 0$ at any finite distances from the surface, as in the MFA. We have seen above that $x_e=1$ for $d=1$ and $x_e\cong 0$ (in fact, $\lambda_e\sim 1$) for $d>4$. Actually, for all values of $x$ one has

$$\Phi(x,0)=\begin{cases}2(1+x), & d=1\\ 2x, & d>4,\end{cases}\tag{4.20}$$

and the curves $\Phi(x,0)$ for all $d$ should go between these straight lines. For $x\ll 1$ in the wide range $y\ll 1/x$ one can write [cf. Eq. (4.9)]

$$\Phi(x,y)\cong\frac{x}{\mu}\left[1-\frac{\Gamma(1-\mu)}{\Gamma(1+\mu)}\left(\frac{xy}{2}\right)^{2\mu}F(y)\right],\tag{4.21}$$

where $\mu=(d-3)/2$ and the scaling function $F(y)$ describes the crossover from the zero $q$ to the isotropic criticality limit at $y\sim 1$ and satisfies $F(\infty)=1$, as well as $F(y)\sim y^{-2\mu}$ for $y\ll 1$. The latter requirement serves to kill the singularity in $q$ for $\kappa\neq 0$; as a result $\sigma_{nn}(\kappa,0)$ behaves similarly to $\sigma_{nn}(0,q)$. For $2<d<3$ one can simply use

$$F(y)\cong\Phi(x\ll 1,y)/\Phi^{\text{isocrit}}(x\ll 1,y) \tag{4.22}$$

to find $F(y)$. The function $\Phi(x,0)$ shows a crossover from $\Phi(x,0)\sim x^{\min(d-2,1)}$ for $x\ll 1$ to $\Phi(x,0)=2(x+x_e)$ for $x\gg 1$ [see Eq. (4.19)].

One can see that only the second, singular, term in Eq. (4.21) makes a $\kappa$-dependent contribution to $\sigma_{nn}^{zz}$ in the limit $q\to 0$. Specifically, for $2<d<4$ one has

$$\chi_{znn}^{\text{sing}}\propto\sigma_{nn}^{zz,\text{sing}}(\kappa,0)\propto n^{d-2}\kappa^{d-3}, \tag{4.23}$$

which in addition shows that the susceptibility increases away from the surface, as it should. In the isotropic case from Eqs. (2.34) and (2.47) it follows that $\kappa\sim\tau^{1/(d-2)}$, thus $\sigma_{nn}^{zz,\text{sing}}(\kappa,0)\sim\tau^{-\gamma_{11}}$ with $\gamma_{11}=(3-d)/(d-2)$ [11]. This result means that the surface susceptibility with respect to the surface field diverges in the ASM only for $d\leqslant 3$. The leading terms of $\chi_{znn}$ near the surface are given by

$$\chi_{znn}\sim\begin{cases} n, & d>3 \\ n\ \ln[1/(\kappa n)], & d=3 \\ n^{d-2}\kappa^{d-3}, & 2<d<3 \\ \kappa^{-1}, & 1\leqslant d<2. \end{cases} \tag{4.24}$$

For the isotropic systems in the range $1\leqslant d\leqslant 2$ the bulk transition temperature is zero. With respect to the latter, $\chi_{znn}$ shows the critical behavior $\chi_{znn}\sim\theta^{-\gamma_{11}}$ with $\gamma_{11}=1/(2-d)$ [see Eqs. (2.34) and (2.47)]. This result is complementary to that for $2<d<4$ quoted above, and it shows similar divergence with $d=2$ approaching from the other side. In the anisotropic case this low-dimensional critical behavior is realized in the range $\tau\gg\tau^*$, where $\tau^*$ is given by Eq. (2.46). In the vicinity of $\theta_c$, i.e., $\tau\ll\tau^*$, the mean-field critical behavior with $\gamma_{11}=-\frac{1}{2}$ is observed.

It should be stressed that the critical amplitudes in the nonscaling region near the surface, $n\sim 1$, cannot be found in the continuous approximation. Here one should numerically solve the ASM equations on the lattice. On the other hand, it can be shown that the critical indices remain unchanged in the nonscaling region. The CFs in this region can be obtained from those in the region $1\ll n\ll 1/\kappa$ with the help of the formulas of type (3.33). Since the quantities $\alpha_n$ and $\alpha_n'$ are all nonsingular, $\sigma_{11}^{zz}$ differs from the result of the continuous approximation extrapolated to $n=1$ by a numerical factor only.

#### *2. The gap tail of the scaling function F(y)*

It turns out that the form (4.17) of the function $g(x)$ for $x\ll 1$ determines the asymptote of the scaling function $F(y)$ of (4.21) for $y\gg 1$, and in the region $x\ll 1$, $y\gg 1$ everything can be calculated analytically. For $y\gg 1$ the solution $\sigma_{nn}$ of Eq. (2.11) at a point $n\ll 1/\kappa$ stems from the interval $|n-n''|\sim 1/q\ll 1/\kappa$ around $n$; thus one can use $g(\kappa n)$ in the form (4.17) and calculate the correction to $\sigma_{nn}$ perturbatively in $a_d(\kappa n)^r$. The resulting expression for the scaling function $\Phi(x,y)$ of Eq. (4.18) has the form

$$\Phi(x,y)\cong 2x[I_\mu(z)K_\mu(z)-Q\Xi_\mu(z)], \tag{4.25}$$

where $z\equiv xy=qn$, the first term corresponds to isotropic criticality,

$$Q\equiv a_d(\tfrac{1}{4}-\mu^2)/y^r\ll 1, \tag{4.26}$$

and the function $\Xi_\mu(z)$ reads

$$\Xi_\mu(z)=K_\mu^2(z)\int_{z_0}^{z}dt\ t^{r-1}[I_\mu^2(t)-c_\mu^2t^{2\mu}]+K_\mu^2(z)\frac{c_\mu^2z^{r+2\mu}}{r+2\mu}$$
$$+I_\mu^2(z)\int_z^\infty dt\ t^{r-1}K_\mu^2(t), \tag{4.27}$$

with $z_0\ll 1$, and $c_\mu\equiv[2^\mu\Gamma(1+\mu)]^{-1}$ is a factor from Eq. (4.8). The part of the expression above without the terms containing $c_\mu$ is just what one obtains from the straightforward perturbative scheme using the Green function (4.2). The additional terms with $c_\mu$ in Eq. (4.27) can be rewritten in the form $K_\mu^2(z)c_\mu^2z_0^{r+2\mu}/(r+2\mu)=CK_\mu^2(z)$, i.e., they can always be added to the solution and their amplitude should be fixed from the boundary condition at the surface. Since this boundary condition is lost in the continuous approximation, the exact form of these terms in Eq. (4.27) has been chosen above from the requirement that the term $CK_\mu^2(z)$, which was ruled out above with the help of the eigenfunction trick, does not appear again in the resulting expression for $\Phi(x,y)$. With such a choice one can set $z_0=0$, because the first integral in Eq. (4.27) converges at the lower limit. Now one can see that the terms with $c_\mu$ cancel each other, if $r+2\mu>0$, whereas in the opposite case they do not. For $\mu<0$ (i.e., $d<3$) the function $\Xi_\mu(z)$ can be rearranged as

$$\Xi_\mu(z)=[2\sin(\pi\mu)/\pi]^2\overline{K}K_\mu^2(z)+\tilde{\Xi}_\mu(z), \tag{4.28}$$

where

$$\tilde{\Xi}_\mu(z)=K_\mu^2(z)\int_0^z dt\ t^{r-1}\tilde{I}_\mu^2(t)+\tilde{I}_\mu^2(z)\int_z^\infty dt\ t^{r-1}K_\mu^2(t),$$

$$\tilde{I}_\mu^2(z)\equiv I_\mu^2(z)-[2\ \sin(\pi\mu)/\pi]^2K_\mu^2(z) \tag{4.29}$$

and

$$\overline{K}=\int_0^\infty dt\ t^{r-1}\left\{K_\mu^2(t)-\left[\frac{\pi}{2\ \sin(\pi\mu)}\right]^2c_\mu^2t^{2\mu}\right\}$$
$$=2^{r-3}\Gamma(r/2+\mu)\Gamma(r/2-\mu)\Gamma^2(r/2)\Gamma^{-1}(r). \tag{4.30}$$

In Eq. (4.30) the subtraction term with $c_\mu$ is present only for $r+2\mu<0$; the resulting expression is valid for both signs of $r+2\mu$. The representation of $\Xi_\mu(z)$ in the form (4.28) for $\mu<0$ is convenient because of the cancellation of the divergence at $t\to 0$ terms in $\tilde{I}_\mu^2(t)$. For $\mu\geqslant 0$ (i.e., $d\geqslant 3$) expression (4.28) remains valid as well, although the subtraction makes little sense and $\Xi_\mu(z)$ can simply be written in the form (4.27) with $z_0=c_\mu=0$.

The parameters $r$ and $a_d$ in Eq. (4.17) should be chosen self-consistently to satisfy the spin-constraint condition. Here

it is convenient to subtract equations (2.65) at and away from isotropic criticality from each other. Thus one can write

$$\int_0^\infty dy\ y^{d'-1}[\Phi^{\rm isocrit}(x,y)-\Phi(x,y)]=M_d, \quad (4.31)$$

where $M_d$ is given by Eq. (2.42). The integral on the left-hand side of Eq. (4.31) is determined by $z=xy\sim 1$, i.e., $y\sim 1/x\gg 1$, which justifies the approximations made above. With the use of Eqs. (4.25) and (4.26) one can rewrite Eq. (4.31) in the form

$$\frac{2a_d(\frac{1}{4}-\mu^2)}{x^{d-2-r}}\int_0^\infty dz\ z^{d-2-r}\Xi_\mu(z)=M_d. \quad (4.32)$$

This equation should be satisfied for all values of $x=\kappa n$, thus

$$r=d-2. \quad (4.33)$$

Then Eq. (4.32) fixes the value of $a_d$:

$$a_d=\frac{2M_d}{(d-2)(4-d)}\bar{\Xi}^{-1}, \quad \bar{\Xi}\equiv\int_0^\infty dz\ \Xi(z). \quad (4.34)$$

The scaling function $F(y)$ in Eq. (4.21) can now be identified taking the limit $z\ll 1$ in Eq. (4.25). This leads to $F(y)\cong 1+2Q\bar{K}\sin(\pi\mu)/\pi$ in the whole interval $2<d<4$. The latter can with the use of Eq. (4.26) be rewritten as

$$F(y)\cong 1+A_d/y^r, \quad y\gg 1, \quad (4.35)$$

where

$$A_d=\frac{\pi^{1/2}\tan(\pi\mu)\Gamma(d-5/2)}{4(d-2)\bar{\Xi}}. \quad (4.36)$$

A remarkable feature of Eq. (4.35) is that the tail of $F(y)$ is, for $d<4$, anomalously long compared to that in the bulk, $F^{\rm bulk}(y)=y^2/\sqrt{1+y^2}\cong 1-1/(2y^2)$. The sign of $A_d$ is determined by $\mu=(d-3)/2$, and one has $A_d=0$ for $d=3$. This is in accord with the structure of Eq. (4.21); in all cases $\Phi(x,y)$ is smaller than $\Phi^{\rm isocrit}(x,y)$, as it should be. In the limit $d\to 4$ the integral $\bar{\Xi}$ of Eq. (4.34) diverges at the upper limit and $A_d$ regularizes to $A_4=\frac{1}{8}$. For $d\to\frac{5}{2}$ the quantity $\bar{K}$ given by Eq. (4.30) diverges, and thus one can neglect $\Xi(z)$ in Eq. (4.28). In this limit $A_d$ regularizes to $A_{5/2}=-4\pi^{1/2}/\Gamma^2(1/4)\approx -0.539$. The same situation takes place for $d\to 2$, where one obtains $A_2=-\frac{1}{2}$. It should be noted, however, that for $d$ close to 2 the tail of $F(y)$ becomes extremely long [see Eq. (4.33)]. The validity of the present approximation for $F(y)$ requires, for $d\to 2$, very large values of $y$, which can become incompatible with the condition $z\equiv xy\ll 1$ needed to represent $\Phi(x,y)$ in the form (4.21). Actually, $d=2$ is a special case with a logarithmically decaying gap tail (see Sec. III B 3).

The quantity $a_d$ given by Eq. (4.34) is positive for $\frac{5}{2}<d<4$ and negative for $2<d<\frac{5}{2}$. At $d=\frac{5}{2}$ one has $a_d=0$ due to the divergence of $\bar{K}$ and hence $\bar{\Xi}$. The latter could raise questions about the validity of the perturbation theory with respect to $a_d(\kappa n)^r$ for $d=\frac{5}{2}$ [should the higher-order terms in Eq. (4.17) be taken into account?]. As we will see below, the numerical results are in excellent agreement with the asymptotic behavior $F(y)\cong 1-0.539/y^{1/2}$ for $d=\frac{5}{2}$ and $y\gg 1$.

## V. NUMERICAL RESULTS

### A. Variation of $G_n$

In the symmetric phase, $m=0$, the ASM equations were solved numerically in the following way. For a given variation of $G_n$ and the value of the wave vector $\mathbf{q}$ in Eq. (2.6), the transverse CF $\sigma_{nn}(\mathbf{q})$ can be found from Eq. (2.5). In practice, the formula (2.63) was used, where $\alpha_{1n}$ and $\alpha'_{1n}$ were determined from the recurrence relations (2.61) and (2.62). The result for $\sigma_{nn}(\mathbf{q})$ can be put into the constraint equation (2.4) to obtain, after the integration over $\mathbf{q}$, the system of nonlinear equations for $G_n$. Again, it is more convenient to work with the deviations from the bulk values and to use the constraint equation in the form (2.65) where the subtraction is done analytically to avoid the loss of accuracy. The integrals over $q$ have been performed in all cases over the whole Brillouin zone, even in low dimensions. For the continuous-dimension model [see Eq. (2.36)] the range $0\leqslant q\leqslant\Lambda$ was divided into three or four log-spaced intervals (e.g., $[0,10^{-4}\Lambda]$, $[10^{-4}\Lambda,10^{-3}\Lambda]$, etc.) and the Gaussian quadratures over 10 or 20 points were used in each of these intervals. For the hypercubic lattice the products of Gaussian quadratures were used, and the intergation was done with respect to the nonlinearly scaled $q$ components $Q_i=q_i^{1/p}$ with $p=3$ to redistribute the contribution of the singularity at $q=0$ more uniformly over the Brillouin zone. In fact, similar nonlinear transformations were also done for the continuous-dimension model. The resulting system of equations for the deviations $G_{1n}$ was solved with a nonlinear equation solver based on the Newton method.

For the numerical solution in the semi-infinite geometry, the boundary condition at $n=\infty$ in Eq. (2.62) should be replaced by one at some $n_{\max}\gg 1$. For the isotropic model at criticality one cannot just set $\alpha'_{1n_{\max}}=0$, since $\alpha'_{1n}$ slowly decays with $n$ [see Eq. (4.15)]. This would spoil the behavior of correlation functions at small wave vectors and lead to an unphysical gap for $2<d\leqslant 3$. Fortunately, the asymptotic behavior of $\alpha'_{1n}$ in the scaling region, $n\gg 1$, is given by Eq. (4.13) with $c'=0$ and it can be used as the boundary condition at infinity. The purpose of numerical calculations at isotropic criticality was to check the scaling solution (4.1) and to study the nonscaling effects at $n\sim 1$. The quantity $\mu$ was determined self-consistently as a function of all $G_{1n}$ using the asymptotic form of $\alpha_{1n}$ at $n\gg 1$ and $q=0$ [see the first limit of Eq. (4.14)]. In this way the value $\mu=(d-3)/2$ has been confirmed.

Above $\theta_c$ or at the anisotropic criticality ($\kappa>0$) the inhomogeneities decay as $\exp(-2\kappa n)$ [see Eq. (4.16)], and one can use the boundary condition $\alpha'_{1n_{\max}}=0$ for $n_{\max}\gg 1/\kappa$. Here the value of $\kappa$ should be taken rather small to study the details of the scaling function $\Phi(x,y)$ in Eq. (4.18). Indeed, to reproduce the limit $x\ll 1$ one should have $\kappa n\ll 1$, where $n^*\sim 10$ is the smallest value of $n$ for which the continuous scaling solution holds. This implies, in turn, large values of

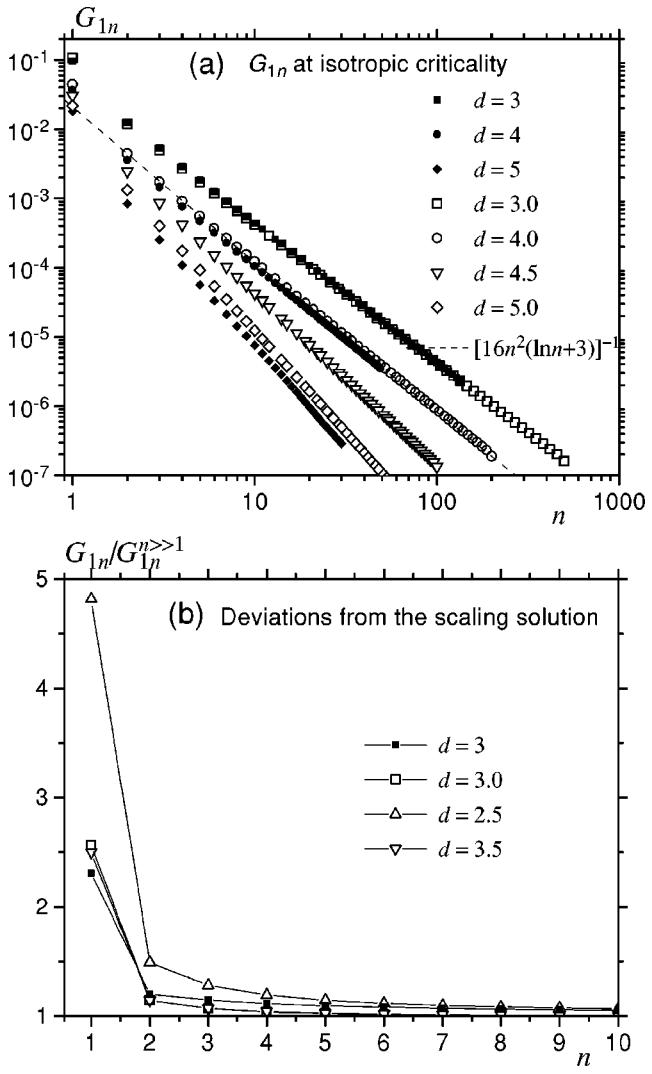


FIG. 1. $G_{1n}$ at isotropic criticality for different hypercubic and continuous-dimension lattices: (a) general view; (b) surface region, deviations from scaling.

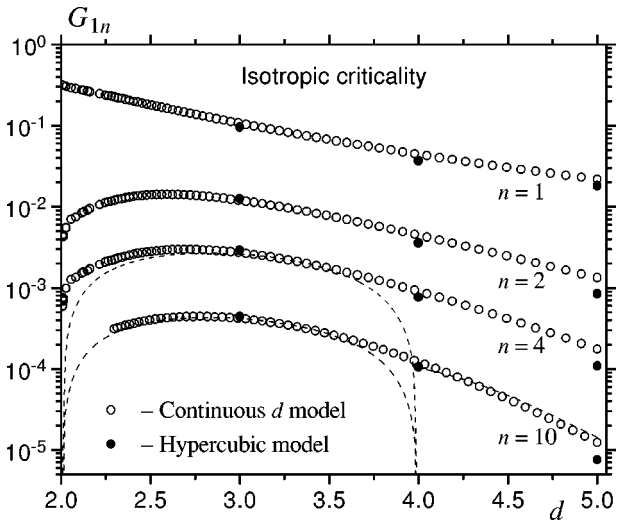


FIG. 2. $G_{1n}$ at isotropic criticality vs lattice dimensionality $d$. The asymptotic scaling result (4.1) for $2<d<4$ and the asymptotic formula (3.43) are shown by dashed lines.

$n_{\max}$. Calculations were done for $1-\eta$ down to $10^{-8}$, which corresponds to $\kappa=\sqrt{2d(1-\eta)}\approx 2.5\times 10^{-4}$ at the anisotropic criticality for $d=3$. For such $\kappa$ the value $n_{\max}=10\,000$ was used, which corresponds to $2\kappa n_{\max}\approx 5$. Naturally, in this case the system of equations for $G_{1n}$ was not solved on each of 10 000 layers. Instead, for $n\gtrsim 10$ only the ''representative'' layers with an exponentially increasing spacing between them were chosen to solve the equations. The values of $G_{1n}$ between them were interpolated with the help of the formula $G_{1n}=(a/n^b)\exp(-2\kappa n)$ with the values of $a$ and $b$ determined from $G_{1n}$ at the ends of the interpolation intervals. In all cases the number of unknowns did not exceed 50. Computations could be performed on a 486DX 66-MHz laptop.

The results for $G_{1n}$, as defined by Eq. (2.12) for *all* values of $n$, are shown at isotropic criticality for different hypercubic and continuous-dimension lattices in Fig. 1. The general view, Fig. 1(a), shows that the analytical result (4.1) is well obeyed in three dimensions outside the surface region. This result is universal and independent of the lattice structure; it is the same for the simple-cubic lattice ($d=3$) and the $3d$ continuous-dimension lattice ($d=3.0$). Formula (4.1) has also been confirmed for other values of $d$ around $d=3$; the results do not differ much from each other in the log scale and thus they have not been shown. In four dimensions the results can be fitted with formula (3.47) with $a=e^3\approx 20$, which implies significant corrections to the logarithmic approximation. In fact, the nonuniversal number $a$ is slightly larger for the hypercubic lattice ($d=3$), which can be seen in Fig. 1(a). In dimensions higher than four, $G_{1n}$ follows formula (3.43). The coefficient in Eq. (3.43) depends on the lattice structure and is clearly different for $d=5$ and $d=5.0$.

Deviations from the asymptotic solution (4.1) in the region near the surface are shown in Fig. 1(b). There is a clear difference between the values of $G_{1n}$ for both three-dimensional lattices.

The dependence of $G_{1n}$ at isotropic criticality near the surface on $d$ is shown in Fig. 2. In the limit $d\to 2$ the value $G_{11}$ tends to $\frac{1}{3}$, which means that the limiting value of $G_1$ is $\frac{4}{3}$, as given by the first term of Eq. (3.9), where, at criticality, $G=1$. On the other hand, all $G_{1n}$ with $n\geqslant 2$ vanish in the limit $d\to 2$, in accord with Eq. (3.15), which disappears for $\kappa\to 0$.

The algorithm for solving the system of nonlinear equations for $G_{1n}$ based on the Newton method, which was used here, shows instability for $d\lesssim 2.3$ and $n_{\max}\gtrsim 10$. This instability is responsible for the lack of points in the left part of the $n=10$ curve. The reason is that the integral in the constraint equation (2.65) becomes more and more sensitive to the region of small $q$ where the integrand may become infinite due to a negative gap arising for some sets of $G_{1n}$ in the course of iterations. Away from isotropic criticality, the gap in the spin CFs stabilizes the algorithm. For each dimension $d$ there is a minimal value of the anisotropy $1-\eta$ for which the system of nonlinear equations for $G_{1n}$ does not show instability for $n_{\max}$ large enough, if the starting variation of $G_{1n}$ is chosen sufficiently close to the actual one. The latter is very important and necessitates using small variations of the parameters, such as $d$, $1-\eta$, $n_{\max}$, etc., in low dimen-

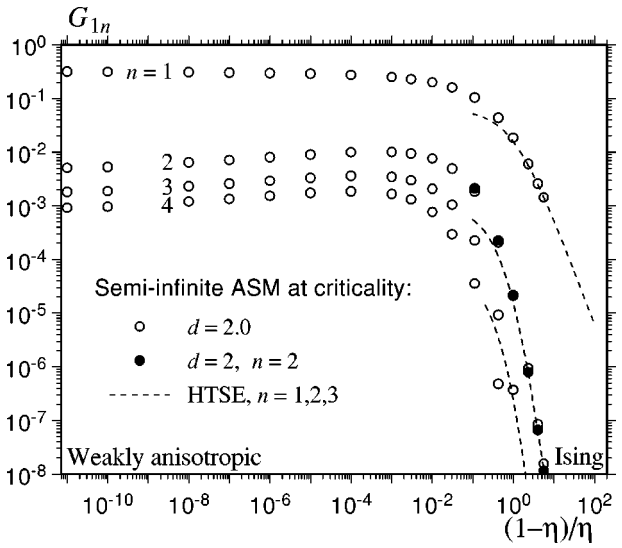


FIG. 3. $G_{1n}$ at the anisotropic criticality in two dimensions vs the anisotropy parameter $\eta$. The HTSE results (2.68) are shown by the dashed lines.

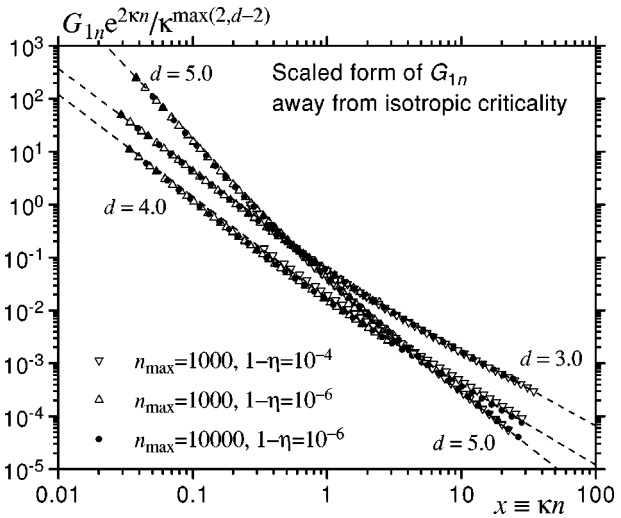


FIG. 4. Scaled form of $G_{1n}$ away from isotropic criticality. Dashed lines are the fits describing crossovers between different power laws.

sions. The minimal values of the anisotropy $1-\eta$ are about $3\times10^{-8}$ for $d=2.0$, $10^{-7}$ for $d=1.75$, and $5\times10^{-7}$ for $d=1.5$.

Contrary to the implication of the scaling solution of Bray and Moore, Eq. (4.1), $G_{1n}$ do not go to zero and do not even show any singularity at $d=4$ for any finite $n$. This is due to the correction-to-scaling terms [see Fig. 1(b)] , which become more and more pronounced as $d$ deviates from 3. The crossover from the solution for $G_{1n}$ in the range $2<d<3$ and that for $d>4$ is described by Eq. (3.46).

Additionally, in four surface layers for the two-dimensional model at criticality, the dependences of $G_{1n}$ on the anisotropy parameter $\eta$ are shown in Fig. 3. Calculations down to $1-\eta=10^{-11}$ were possible here, since the value of $n_{\max}$ was chosen to be about 50, which is significantly smaller than the required $n_{\max}\gg1/\kappa$. The latter introduces a significant gap in the spin CFs, which is the artifact of cutting the ASM equations at $n_{\max}\lesssim1/\kappa$. This gap stabilizes the solution of the ASM equations. On the other hand, the values of $G_{1n}$ in several layers near the surface are pretty robust and insensitive to this defect of $\sigma_{nn}$. One can see that in the isotropic limit, $\eta\to1$, the value of $G_{11}$ tends to $\frac{1}{3}$, whereas all other $G_{1n}$ tend to zero logarithmically in accordance with Eq. (3.15). In the opposite limit, $\eta\ll1$, the HTSE results (2.68) are recovered.

In Fig. 4 the calculated values of $G_{1n}$ for continuous-dimension lattices away from the isotropic criticality are represented in the scaled form. The results for $d=5.0$ show crossover from Eq (3.43) to Eq (3.44) as $x\equiv\kappa n$ increases. A similar crossover from $G_{1n}\sim1/n^2$ to $G_{1n}\sim e^{-2\kappa n}/n^{3/2}$ takes place for $d=4.0$. The scaling is, however, not perfect here because of the logarithmic corrections. For $d=3.0$ the result crosses over to $G_{1n}\sim e^{-2\kappa n}/n^{1.4}$ for $\kappa n\gg1$. Note that there is no analytical solution for $G_{1n}$ in this region.

The calculated values of $G_{1n}$ at the anisotropic criticality (or above criticality) in low dimensions ($d=1.5$, 1.75, and 2) are shown in Fig. 5. One can see that the theoretical formulas (3.14) and (3.15) are obeyed starting from $n\gtrsim10$, although corrections related to the finite value of $\kappa$ and described by the function $g(\kappa n)$ in Eq. (3.16) are quite pronounced. For $d=2.0$ the function $g(\kappa n)$ is nonmonotonic: apart from the exponential decrease at $\kappa n\gg1$ it shows a singular positive deviation from unity for $\kappa n\ll1$. The fit in Fig. 6 suggests $g(\kappa n)\cong1+2\sqrt{\kappa n}$ for $\kappa n\ll1$. One can see from Fig. 5 that the correction term in $g(\kappa n)$ has the negative sign for $d=1.5$. The case $d=1.75$ seems to be marginal. The values of $G_{1n}$ in Fig. 5 nicely follow the dependence $G_{1n}=G_{1n}^{\text{approx}}$, where $G_{1n}^{\text{approx}}$ is given by Eq. (3.14) with the additional factor $\exp(-2\kappa n)$ in the whole range of $n$. This is, however, not an exact solution to the problem. The plot of $G_{1n}/G_{1n}^{\text{approx}}$ in Fig. 7 shows that for $\kappa n\gtrsim1$ this function begins to increase with oscillations. These oscillations are not an artifact of cutting the ASM equations at the maximal layer number $n_{\max}$. Numerical calculations with different values of $n_{\max}$ give the same results. Although the ratio $G_{1n}/G_{1n}^{\text{approx}}$ is not exactly 1, its proximity to 1 in a wide range of $n$ is remarkable, taking into account the strong dependence of $G_{1n}$ on $n$.

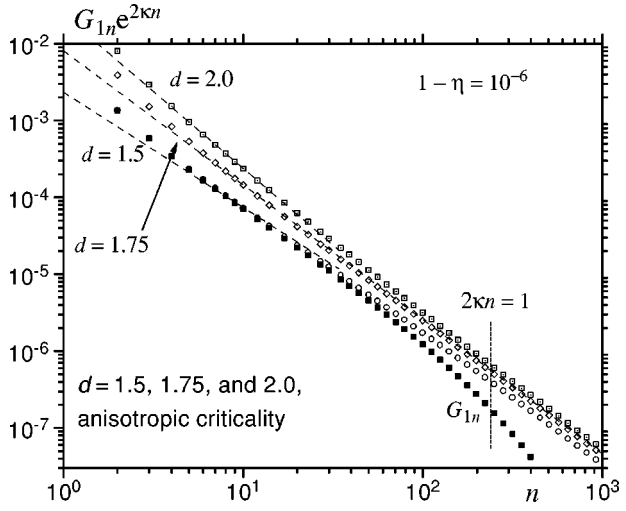


FIG. 5. $G_{1n}$ in low dimensions at the anisotropic criticality. Dashed lines represent the theoretical formulas (3.14) and (3.15), the latter with the fitting parameter $a=e=2.718$.

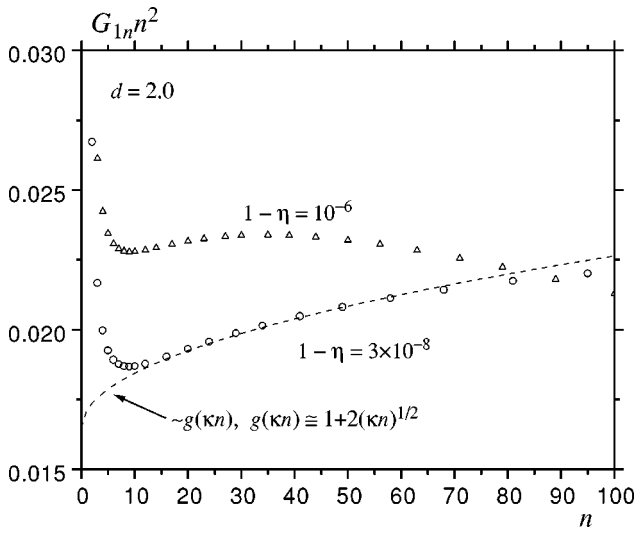


FIG. 6. $G_{1n}$ for $d=2.0$ at the anisotropic criticality: scaling function $g(\kappa n)$ and deviations from scaling near the surface.

### B. Correlation functions

After $G_{1n}$ has been determined, the spin CFs can be found from Eq. (2.63) and the recurrence relations (2.61) and (2.62). The results at isotropic criticality in the scaling region $n \gg 1$, which illustrate the analytical solution of Bray and Moore (4.2) for $2<d<4$, are shown in Fig. 8. One can see that for $2<d<4$ the solution satisfies $\sigma_{nn}<\sigma_{nn}^{\text{bulk}}$ for small wave vectors and $\sigma_{nn}>\sigma_{nn}^{\text{bulk}}$ for large wave vectors. For $d=4$ one has $\sigma_{nn}<\sigma_{nn}^{\text{bulk}}$ everywhere, which contradicts the constraint equation (2.65). In fact, for $d \geqslant 4$ the scaling solution of Bray and Moore breaks down, and one has to take into account the *positive* local contribution to $\sigma_{nn}$ at $q \sim 1$ [see Eq. (3.40)], which balances the constraint equation. For $d=2$ one has $\sigma_{nn}>\sigma_{nn}^{\text{bulk}}$ everywhere, and the constraint relation is violated again. In fact, for $d \leqslant 2$ the form of $\sigma_{nn}$ is changed by the gap in the region of small $q$, where $\sigma_{nn}<\sigma_{nn}^{\text{bulk}}$, thus ensuring the constraint (see Fig. 10).

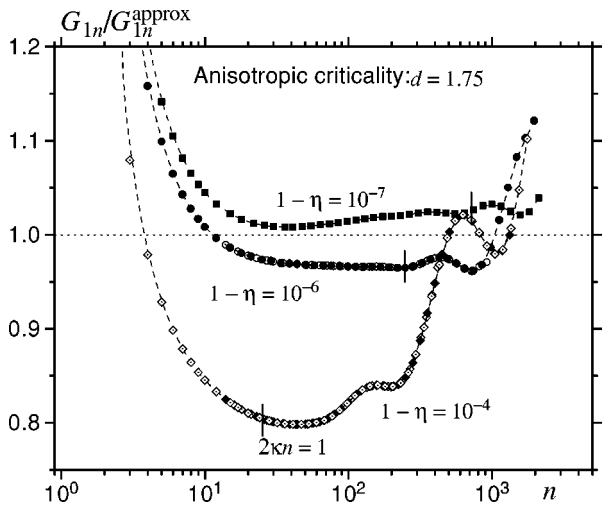


FIG. 7. $G_{1n}$ for $d=1.75$ relative to its approximation shown by the dashed line in Fig. 5. Overlapping solid and open symbols correspond to different values of the maximal number of layers $n_{\max}$ in the numerical calculation.

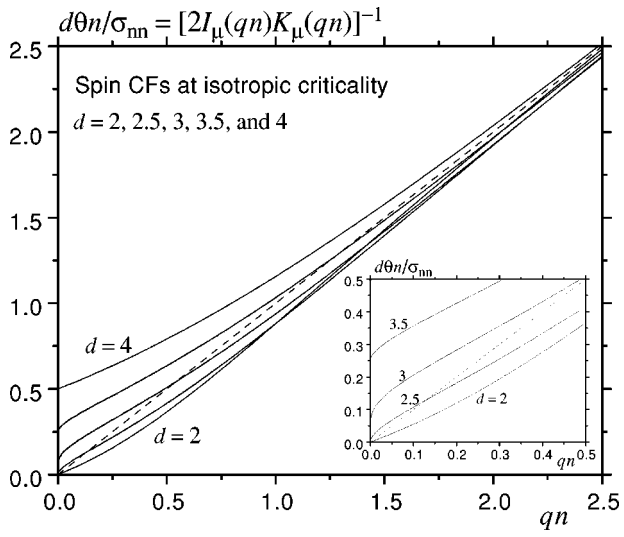


FIG. 8. Reciprocal of the spin CFs at isotropic criticality in the scaling region $n \gg 1$ for different lattice dimensionalities $d$. The dashed line is the bulk solution (2.33).

Deviations from the scaling solution (4.2) in the region near the surface, $n \sim 1$, are shown in Fig. 9. The correlation functions in different layers are related to each other by Eq. (3.33), where the quantities $\alpha_n$ and $\alpha_n'$ are constants in the limit $q \to 0$ and they approach the bulk value $\alpha$ of Eq. (2.32) with increasing $n$. For $n \gg 1$ small deviations of $\alpha_n$ and $\alpha_n'$ from $\alpha$ are responsible for the scaling form of $\sigma_{nn}$ showing only a small change when $n$ changes by one. By contrast, in the nonscaling region, $n \sim 1$, the spin CFs change significantly from one layer to another and they acquire in the range $q \ll 1$ nonuniversal numerical factors, relative to the extrapolated scaling solution. These factors, which are shown in Fig. 9, tend to 1 as some negative powers of $n$ far from the surface. The accuracy of the calculations is, however, not high enough to determine these powers precisely. One can see that the deviations from scaling are quite large and slowly decaying for the dimensions well above 3 [cf. Eq. (3.46)]. On the other hand, for $d$ well below 3 the deviations from scaling are mainly localized near the surface. Note the

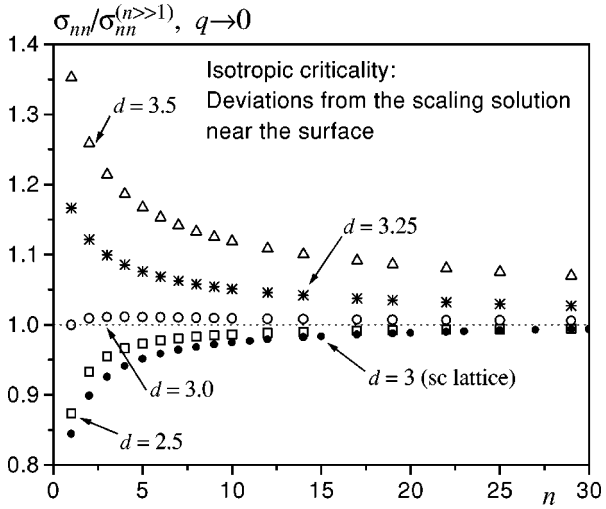


FIG. 9. Deviations from the scaling solution (4.2) for $\sigma_{nn}$ in the nonscaling region $n \sim 1$.

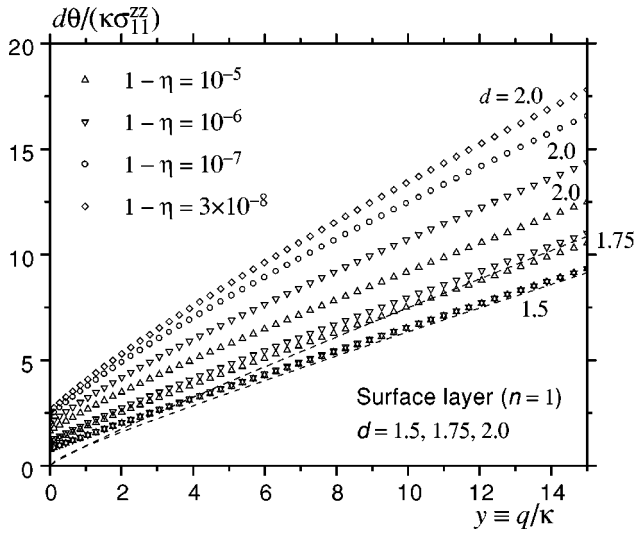


FIG. 10. Reciprocal of the longitudinal CF $\sigma_{nn}^{zz}$ in the surface layer ($n=1$) in low dimensions at anisotropic criticality. Dashed lines represent the asymptote $[q+\overline{\Delta}_1(q,\kappa)]/2$ with $\overline{\Delta}_1(q,\kappa)$ given by Eq. (3.31) for $q \gg \kappa$.

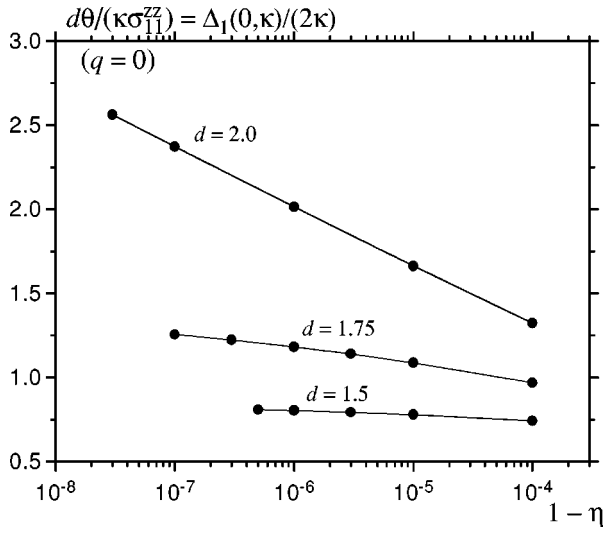


FIG. 11. Dependence of the gap in $\sigma_{11}^{zz}$ on the anisotropy at anisotropic criticality in low dimensions.

difference between the results for the simple-cubic ($d=3$) lattice and the three-dimensional continuous-dimension lattice ($d=3.0$). For the latter the deviations from scaling are anomalously small, which suggests the existence of an exact solution. If one assumes that the scaling form of $\sigma_{nn}$ holds for all $n$, then from Eqs. (3.33) and (2.55) it follows that $\alpha_n=\sqrt{1-1/n}$ and $\alpha_n'=\sqrt{1+1/n}$ for $q=0$. Then, using the divergence of Eq. (2.53) for $q\to0$ one obtains

$$G_n=\frac{6}{4+\sqrt{1+1/n}+\sqrt{1-1/n}}, \quad d=3.0, \tag{5.1}$$

which is indeed a rather good approximation. It has the proper behavior $G_n\cong1+1/(24n^2)$ for $n\gg1$, and the value $G_1=1.1082$ is very close to 1.1067 following from numerical calculations. More careful analysis shows, however, that the formula above is not an exact solution for the ASM equations, where discrepancies of the type $\sqrt{2}\,\ln 2\approx0.980\neq1$ arise.

At anisotropic criticality, which is the only type of criticality in low dimensions, the generic CF is $\sigma_{nn}^{zz}$. The transverse CF $\sigma_{nn}$, as well as $\sigma_{nn}^{zz}$ itself above criticality, can be obtained from the latter by the simple change of the wave-vector argument. The numerical results for $\sigma_{nn}^{zz}$ in the surface layer ($n=1$) at anisotropic criticality in low dimensions are shown in Fig. 10. One can see the gap and the linear $q$ dependence at small $q$, in accord with Eq. (3.29). The values of the gap $\Delta_1(0,\kappa)$ and the stiffness $A$ in Eq. (3.29) determined from the fits of the numerical data exceed those calculated from Eqs. (3.28) and (3.30). The reason for this is that the first-order perturbation theory in $G_{1n}$ leading to Eqs. (3.28) and (3.30) is valid for small wave vectors only in the dimension range $d<1.5$, as was explained after Eq. (3.22). On the other hand, the asymptote $\overline{\Delta}_1(q,\kappa)$ for $q\gg\kappa$, which is given by Eq. (3.31), works nicely for $d=1.5$ and $d=1.75$.

It can be seen that for $d=1.5$ the results for the models with different anisotropies scale with each other. This confirms the concept of the strong scaling (down to the surface layer) in low dimensions, which has been suggested in Sec. III B 2. For $d=1.75$ the scaling in Fig. 10 is incomplete, which can be explained by the values of $\kappa$ not being small enough. For $d=2.0$ the results do not scale, although they do not deviate far from each other, because $d=2$ is the marginal dimension between the strong scaling and the asymptotic ($n\gg1$) scaling. This behavior is illustrated in greater detail in Fig. 11, where the gap $\Delta_1(0,\kappa)$ of $\sigma_{11}^{zz}$ is plotted as a function of the anisotropy. Whereas the dependences for $d=1.5$ and $d=1.75$ saturate in the limit of $\kappa\equiv\sqrt{2d(1-\eta)}$ going to zero, which confirms $\Delta_1(0,\kappa)\propto\kappa$ for weakly anisotropic models, the almost perfectly straight line over several decades for $d=2.0$ suggests $\Delta_1(0,\kappa)\propto\kappa\,\ln(1/\kappa)$ in two dimensions.

The numerical result for $d=2$ above is quite plausible, because logarithms usually arise in marginal dimensions. This would imply something like $\chi_{znn}\propto\kappa^{-1}/\ln[1/(\kappa n)]$ for $d=2$ in Eq. (4.24), where the corresponding position has been left empty. It seems to be, however, the third occasion in this work when numerical calculations suggest some qualitative features that do not follow from analytical considerations. For $d=2$ the calculation with logarithmic accuracy leads to another dependence of $\Delta_1(0,\kappa)$, which is given by Eq. (3.37). The applicability of Eq. (3.37) requires, however, such small values of the anisotropy that numerical calculations cannot be performed, and for larger anisotropies no other possible analytical approximations are seen.

To shed some light on this puzzle, it is convenient to plot $q^{d-1}\sigma_{nn}$ as a function of $\log q$ over the whole Brillouin zone. The area under the curve is proportional to the integral over $q$ in the constraint equation (2.65), and the regions of $q$ making contributions into the constraint can be well identified. Such plots show that the integral is dominated by $q\sim1/n$ for $d>2$ and by $q\sim\kappa$ for $d<2$. In the marginal case $d=2$ the results for the lowest manageable anisotropy, $1-\eta=3\times10^{-8}$, are shown in Fig. 12. One can see that the area under the bulk solution (the solid line) coincides with

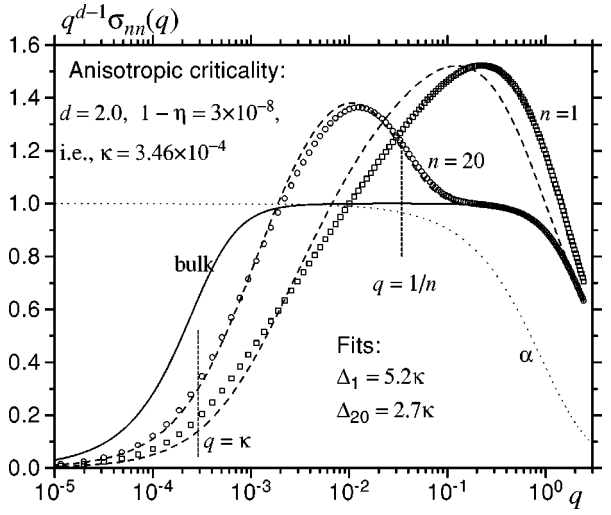


FIG. 12. Transverse CF $\sigma_{nn}$ in two dimensions. Circles: numerical results for $n=1$ and $n=20$. Dashed lines: Bessel-function solution with fitted gap, as explained in the text.

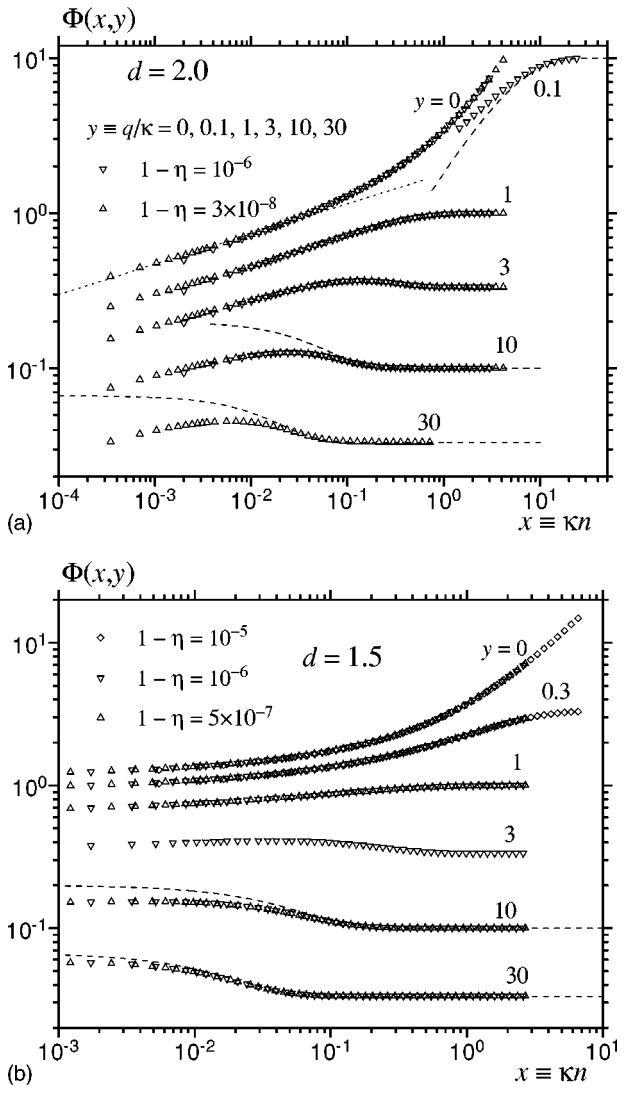


FIG. 13. Scaling representation of $\sigma_{nn}^{zz}$ for $d=2$ and $d=1.5$. Dashed lines: free solutions $\Phi(x,y)=(1\pm e^{-2xy})/y$ for large and small values of $y$.

that under the numerical solutions for $n=1$ and $n=20$ (open circles). The curve for $n=20$ merges with the bulk curve for $q \gtrsim 1/n$. Although the distance between $q\sim1$ or $q\sim1/n$ on the right-hand side and $q\sim\kappa$ on the left-hand side is several decades, it is not large enough to apply the logarithmic approximation, i.e., to integrate the solution obtained for $\kappa \ll q \ll 1/n$ between these limits. The applicability condition for the formula (3.37) is clearly not satisfied. Nevertheless, as we have seen in Fig. 5, formula (3.15) is in reasonable agreement with the numerical results for $G_{1n}$ for small $\kappa n$. Thus one can use the solution (4.2) for $\sigma_{nn}$ in terms of the modified Bessel functions of index $\mu$ given by Eq. (3.35). This solution with $\tilde{q} \Rightarrow \tilde{q} + \Delta_n(0,\kappa)$ is plotted with dashed lines in Fig. 12, where the gap values $\Delta_1(0,\kappa)=5.2\kappa$ (taken from Fig. 11) and $\Delta_{20}(0,\kappa)=2.7\kappa$ were used as fitting parameters. The agreement with numerical results is rather good. On the other hand, $1/\ln(1/\kappa)$ is not small enough to use the simplified form (3.36) for $\sigma_{nn}$. The corresponding curves deviate strongly from the numerical solution in Fig. 12, thus the final result (3.37) is not realized. And analytically calculating the constraint integral with the gapped Bessel functions to obtain the simple empirical formula $\Delta_1(0,\kappa) \propto \kappa \ln(1/\kappa)$ seems to be impossible.

Now let us consider the numerical results for the longitudinal CF $\sigma_{nn}^{zz}$ in the scaling representation (4.18). The scaling function $\Phi(x,y)$ for $d=2.0$ and 1.5 is represented in Fig. 13. One can see that the asymptotic scaling (for $n \gg 1$) is well obeyed. For $d=2$ in the surface region $n\sim1$ there are small, seemingly logarithmic deviations from the strong scaling, as was suggested above for the two-dimensional model. Here, for small $x$ the results can be fitted with power-law functions, the exponent slowly decreasing with $\kappa$. In particular, for $1-\eta=3\times10^{-8}$ this exponent is 0.195, which roughly agrees with $1/\ln(1/\kappa)=0.125$ following from Eq. (3.36). For large and small values of $y$ the numerical results contain the features of the free solution $\Phi(x,y)=(1\pm e^{-2xy})/y$, as was argued in Sec. III B 2. In fact, $d=2$ is a marginal dimension, and for $d<2$ the free solution is reproduced for large and small $y$ much better, as can be seen from the plot for $d=1.5$. The latter also confirms the strong scaling in low dimensions.

The results for $\Phi(x,0)$ in the whole range of lattice dimensions are shown in Fig. 14. All the curves are bounded by the ones representing the exact expressions of Eq. (4.20). For small $x$ the results are in accord with Eq. (4.24). The asymptotic form of the curves in the region $x \gg 1$, which is given by the limit $y\to0$ of (4.19), determines the extrapolation length $\lambda_e$. The latter is represented in Fig. 15 as a function of $d$. One can see that for $d<4$ the extrapolation length is of the order of transverse correlation length $\xi_{c\alpha}$, which is a ''mesoscopic'' length scale between the lattice spacing $a_0$ and the diverging longitudinal correlation length $\xi_{cz}$.

For $d>2$ the scaling form of the correlation function holds in the asymptotic region $n \gg 1$. The general view of the scaling function $\Phi(x,y)$ is shown for $d=3.0$ in Fig. 16. One can figure out how the results look like for other dimensions with the help of Figs. 13 and 14. The results for the wave-vector scaling function $F(y)$ defined by Eq. (4.21) or, for $2<d<3$, also by Eq. (4.22), are shown for $d=2.5$ in Fig. 17. The dimension $d=2.5$ is especially convenient since here the

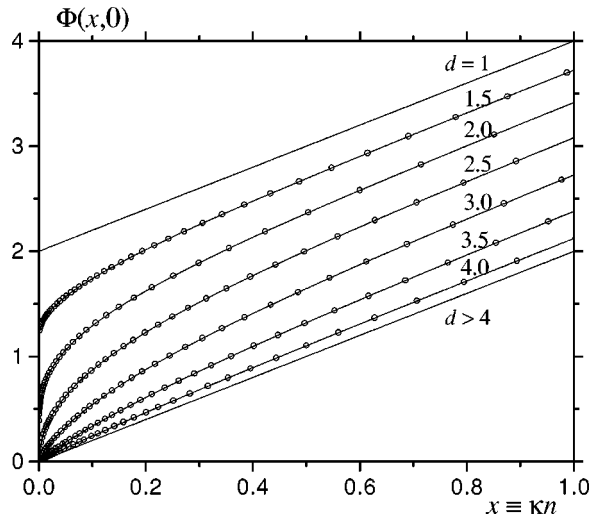


FIG. 14. Scaling function at zero wave vector, $\Phi(x,0)$, in all dimensions.

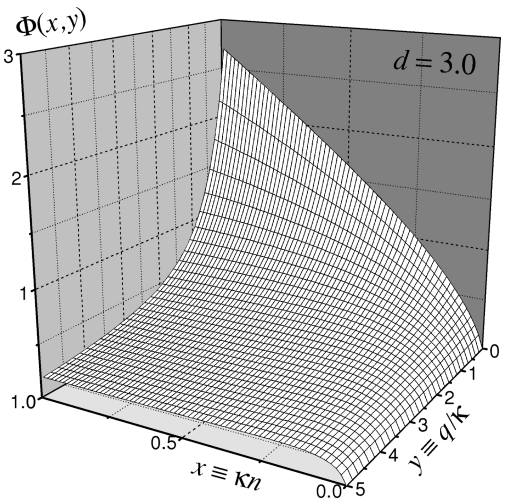


FIG. 16. Scaling function $\Phi(x,y)$ of (4.18) for $d=3$.

coefficient $A_d$ in the gap tail of $F(y)$ given by Eq. (4.35) simplifies to $A_{5/2}=-4\pi^{1/2}/\Gamma^2(1/4)\approx-0.539$. In order to reduce the value of $z=xy=qn$, which should be small according to the definition of $F(y)$, the solution for the CF in the first two layers has been used. Calculation of $F(y)$ with the help of Eq. (4.22) yields the curves of solid triangles in Fig. 17. These curves do not scale with each other, because strong scaling does not hold for $d\geqslant 2$. Nevertheless, correlation functions in the asymptotic region $n\gg 1$ differ from those in the nonscaling region near the surface only by numerical factors, which are represented in Fig. 9. Inserting these factors into $F(y)$ makes the results for $n=1$ and $n=2$ scale. These corrected results are in excellent accord with the asymptotic formula (4.35) for $y\gg 1$.

The longitudinal CF $\sigma_{nn}^{zz}$ itself, which also is shown in Fig. 17, has the same cusplike form with a gap described by Eq. (3.29), as in low dimensions. The linear $q$ dependence in the denominator of Eq. (3.29) says that, in spite of the gap, the correlation length of $\sigma_{nn}^{zz}$ near the surface is infinite at the anisotropic criticality. Actually, the correlation lengths near the surface are, in the ASM, the same as in the bulk. Indeed, above criticality $\sigma_{nn}^{zz}$ is a function of $\tilde{q}_z=\sqrt{\kappa_z^2+q^2}$; thus there are singularities in $\sigma_{nn}^{zz}$ at $q=\pm i\kappa_z$, which cause the decrease of correlations of the type $\exp(-\kappa_z r)$ in the real space at large distances.

## VI. DISCUSSION

In this paper, a comprehensive analysis of the behavior of the semi-infinite anisotropic spherical model at and above the ordinary phase transition is presented. The critical coupling of fluctuations, which usually necessitates application of the $\epsilon$ expansion or purely numerical methods, dies out in this model due to the infinite number of spin components and makes it exactly solvable. On the other hand, the more important *qualitative* effects associated with Goldstone or quasi-Goldstone modes in weakly anisotropic magnetic systems are properly described by the ASM. The most important of these effects is the anisotropy-induced ordering in low dimensions. The ASM is superior with respect to the usual spherical model, which cannot incorporate anisotropy and yields unphysical results for spacially inhomogeneous systems because of the global spin constraint. On the other

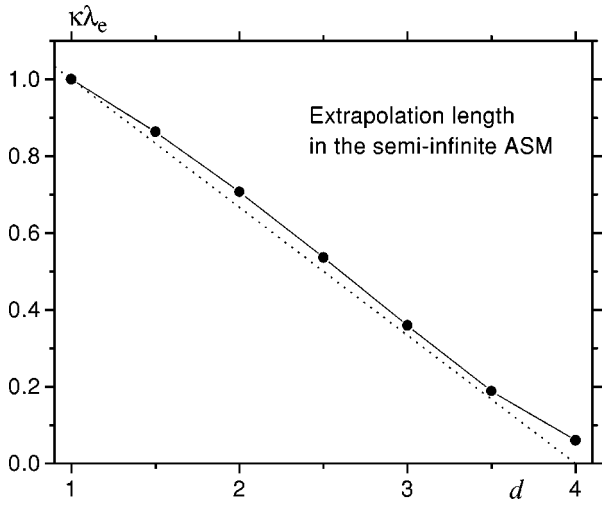


FIG. 15. Extrapolation length vs lattice dimension.

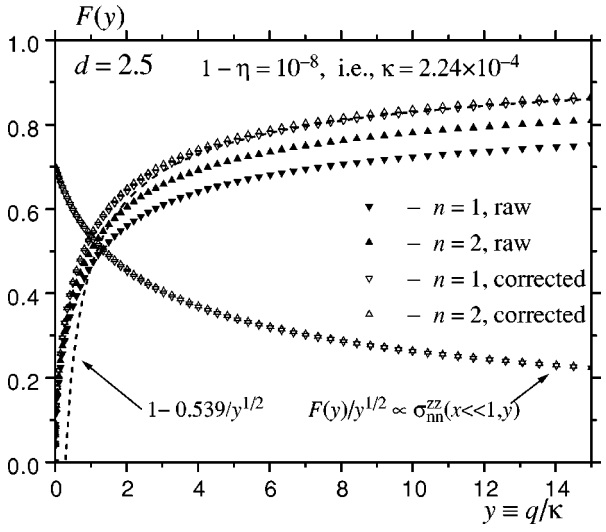


FIG. 17. Scaling function $F(y)$ of (4.22) for $d=2.5$.

hand, the ASM is much better defined than its phenomenological field-theoretical analog, the infinite-component $\phi^4$ model, and it can always be solved numerically.

Unlike the renormalization-group (RG) approach, which is based on the expansion about the dimension $d=4$ and becomes inefficient for low dimensions, the ASM describes the whole range $1 \leqslant d \leqslant \infty$ in a uniform way. The price for that is the rather complicated character of the ASM system of equations in constrained geometries, which makes application of numerical methods necessary. Nevertheless, there are a number of analytical solutions of the semi-infinite ASM in different limiting and particular cases. The most important of them are the isotropic-criticality solution of Bray and Moore for $2<d<4$, which was obtained above in and easier and more general way, the variations of the gap parameter $G_{1n}$ for $d \leqslant 2$ and $d \geqslant 4$, and the slowly decaying gap tails of the correlation functions for $q \gg \kappa$ away from isotropic criticality.

The gap parameter $G_n$, or its deviation from the bulk value $G_{1n}$, plays a fundamental role in the theory of ASM. The quantity $-G_{1n}$ is similar to the function $V(z)$ used by Bray and Moore, and it also is proportional (and at criticality equal) to the inhomogeneity of the energy density, $\tilde{U}_{1n}$ [see Eq. (2.23)]. The latter has been determined in Ref. [10] using renormalization-group and scaling arguments with the result $\tilde{U}_{1n} \propto 1/n^{(1-\alpha)/\nu}$ for $2<d<4$ at isotropic criticality, where $\nu$ and $\alpha$ are the bulk correlation length and the heat capacity exponents. In the ASM $\nu=2/(d-2)$, as follows from Eqs. (2.34) and (2.47), and $\alpha=(d-4)/(d-2)$, as follows from Eqs. (2.22) and (2.47). Thus the above formula reduces to $G_{1n} \cong \tilde{U}_{1n} \propto 1/n^2$, as was obtained by Bray and Moore. In these approaches, which consider $n$ as a continuous variable, the inhomogeneous part of the energy shows strong and unphysical divergence at the surface. Although it is clear that the continuous approximation is generally invalid near the surface, this strong singularity does not allow one to avoid the problem by replacing the surface region by some effective boundary condition, as can be done in the MFA. As a result, a numerical solution is principally ruled out for the semi-infinite field-theoretical $O(\infty)$ model. In contrast, no such problems arise in the ASM, which is formulated on the lattice from the beginning. Moreover, continuous dimensionalities (in the directions parallel to the surface) can be introduced into the ASM as well, while preserving the semi-infinite dimension discrete. The consideration in this paper shows that the nonscaling region near the surface, $n \sim 1$, plays a very important role in the behavior of the CFs in the asymptotic region far from the surface. So, the isotropic-criticality CFs are different for, say, $d=2.5$ and $d=3.5$, although they satisfy the same equation in the region $n \gg 1$. The difference between them stems completely from the region $n \sim 1$.

The universality of the physical quantities in the ASM is different in different dimensionality ranges. For $d>4$ the gap parameter $G_{1n}$ is nonuniversal and decays as $1/n^{d-2}$, although the CFs have the universal mean-field form for $n \gg 1$. For $2<d<4$ both $G_{1n}$ and CFs are universal for $n \gg 1$ and nonuniversal for $n \sim 1$. For $d<2$ the values of $G_{1n}$ are universal and decay as $1/n^d$ for $n \gg 1$. In contrast, the correlation functions are universal in the whole range of $n$. The reason for this strong universality and the ensuing strong scaling is that the (transverse) CFs satisfy the constraint equation containing the integral over the wave vector $q$ dominated by $q \sim \kappa \ll 1$ in low dimensions.

The next steps in studying the inhomogeneous magnetic systems with the help of the ASM should be (i) the solution of the semi-infinite problem below $T_c$ and in field, (ii) inclusion of surface terms in the Hamiltonian, and (iii) numerical solution of the model in the film geometry. The preliminary analytical investigation of the last problem can be found in Ref. [34].


[1] D. L. Mills, Phys. Rev. B **3**, 3887 (1971).
[2] T. Wolfram, R. E. Dewames, W. F. Hall, and P. W. Palmberg, Surf. Sci. **28**, 45 (1971).
[3] M. I. Kaganov and A. M. Omelyanchouk, Zh. Éksp. Teor. Fiz. **61**, 1679 (1971) [Zh. Eksp. Teor. Fiz. **34**, 895 (1972)].
[4] K. Binder and P. C. Hohenberg, Phys. Rev. B **6**, 3461 (1972); **9**, 2194 (1974).
[5] T. C. Lubensky and M. H. Rubin, Phys. Rev. B **12**, 3885 (1975).
[6] K. Binder, Physica (Amsterdam) **62**, 508 (1972).
[7] M. E. Fisher and M. N. Barber, Phys. Rev. Lett. **28**, 1516 (1972).
[8] T. C. Lubensky and M. H. Rubin, Phys. Rev. Lett. **31**, 1469 (1973); Phys. Rev. B **1**, 4533 (1975).
[9] H. W. Diehl and S. Dietrich, Z. Phys. B **42**, 65 (1981).
[10] S. Dietrich and H. W. Diehl, Z. Phys. B **43**, 315 (1981).
[11] K. Binder, in *Phase Transitions and Critical Phenomena*, edited by C. Domb and J. L. Lebowitz (Academic Press, New York, 1983), Vol. 8.
[12] M. N. Barber, in *Phase Transitions and Critical Phenomena* (Ref. [11]), Vol. 8.
[13] M. Krech, E. Eisenriegler, and S. Dietrich, Phys. Rev. E **52**, 1345 (1995).
[14] E. Eisenriegler, M. Krech, and S. Dietrich, Phys. Rev. B **53**, 14 377 (1996).
[15] B. M. McCoy and T. T. Wu, Phys. Rev. **162**, 346 (1967).
[16] M. E. Fisher and A. E. Ferdinand, Phys. Rev. Lett. **19**, 169 (1967).
[17] H. Au-Yang and M. E. Fisher, Phys. Rev. B **21**, 3956 (1980).
[18] L. V. Mikheev and M. E. Fisher, Phys. Rev. Lett. **70**, 186 (1993); Phys. Rev. B **49**, 378 (1994).
[19] Yi Li and K. Baberschke, Phys. Rev. Lett. **68**, 1208 (1992).
[20] P. Schilbe, S. Siebentritt, and K.-H. Rieder, Phys. Lett. A **216**, 20 (1996).
[21] K. Baberschke, Appl. Phys. A: Mater. Sci. Process. **62**, 417 (1997).
[22] H. E. Stanley, Phys. Rev. Lett. **20**, 589 (1968).
[23] H. E. Stanley, in *Phase Transitions and Critical Phenomena* (Ref. [11]), Vol. 3.
[24] H. E. Stanley, Phys. Rev. **176**, 718 (1968).
[25] T. N. Berlin and M. Kac, Phys. Rev. **86**, 821 (1952).

[26] M. N. Barber and M. E. Fisher, Ann. Phys. (N.Y.) **77**, 1 (1973).
[27] H. J. F. Knops, J. Math. Phys. **14**, 1918 (1973).
[28] G. Costache, D. Mazilu, and D. Mihalache, J. Phys. C **9**, L501 (1976).
[29] S. Allen and R. K. Pathria, J. Phys. A **26**, 6797 (1993).
[30] A. E. Patrick, J. Stat. Phys. **75**, 253 (1994).
[31] S. Allen, J. Stat. Phys. **79**, 165 (1995).
[32] D. M. Danchev, J. G. Brankov, and M. E. Amin, J. Phys. A **30**, 5645 (1997).
[33] D. A. Garanin, J. Phys. A **29**, 2349 (1996).
[34] D. A. Garanin, J. Phys. A **29**, L257 (1996).
[35] L. N. Bulaevskii and V. L. Ginzburg, Zh. Éksp. Teor. Fiz. **45**, 772 (1963) [JETP **18**, 530 (1964)].
[36] J. J. van den Broek and H. Zijstra, IEEE Trans. Magn. **MAG-7**, 226 (1971).
[37] S. Sarker, S. E. Trullinger, and A. R. Bishop, Phys. Lett. A **59**, 255 (1976).
[38] J. J. Niez, J. Phys. C **9**, 2933 (1976).
[39] J. Lajzerowicz and J. J. Niez, J. Phys. (France) **40**, L165 (1979).
[40] I. D. Lawrie and M. J. Lowe, J. Phys. A **14**, 1981 (1981).
[41] D. A. Garanin, Physica A **172**, 470 (1991).
[42] D. A. Garanin, Physica A **178**, 467 (1991).
[43] J. Kötzler, D. A. Garanin, M. Hartl, and L. Jahn, Phys. Rev. Lett. **71**, 177 (1993).
[44] M. Hartl-Malang, J. Kötzler, and D. A. Garanin, Phys. Rev. B **51**, 8974 (1995).
[45] D. B. Abraham and M. A. Robert, J. Phys. A **13**, 2229 (1980).
[46] N. Angelescu, M. Bundaru, and G. Costache, J. Phys. A **14**, L533 (1981).
[47] D. A. Garanin, Z. Phys. B **102**, 283 (1997).
[48] A. J. Bray and M. A. Moore, Phys. Rev. Lett. **38**, 735 (1977); J. Phys. A **10**, 1927 (1977).
[49] D. A. Garanin and V. S. Lutovinov, Solid State Commun. **50**, 219 (1984).
[50] D. A. Garanin, J. Stat. Phys. **74**, 275 (1994).
[51] D. A. Garanin, Phys. Rev. B **53**, 11 593 (1996).
[52] K. M. Case, Phys. Rev. **80**, 797 (1950).